Physics – Uspekhi **49** (5) 469 – 487 (2006)

REVIEWS OF TOPICAL PROBLEMS PACS numbers: **82.39.–k**, **87.50.–a**, 87.50.Gi, 87.54.Br

The mechanism for the primary biological effects of ionizing radiation

V M Byakov, S V Stepanov

DOI: 10.1070/PU2006v049n05ABEH005783

Contents

Abstract. **The primary biological response of living organisms to the passage of fast charged particles is traditionally believed to be dominated by the chemical reactions of the radical products from the radiolysis of cellular water (OH, H, e^-_{aq}, O^-_2, H_2O_2) and by the bioradicals that they produce (and which can also result from the direct electronic activation of biomolecules). This understanding has provided insight into how ionizing radiations affect biological systems and, most importantly, what radioprotection and radiosensibilizing effects are produced by chemical compounds introduced into an organism. However, a number of key radiobiological facts remain unexplained by the current theory, stimulating a search for other biologically active factors that may be triggered by radiation. This review examines a fact that is usually ignored in discussing the biological impact of ionizing radiation: the local increase in acidity in the water solution along the track of a charged particle. The acidity in the track is very different from its value for cellular water in a living organism. Biological processes are well-known to be highly sensitive to changes in the environmental acidity. It seems that the biological impact of ionizing radiations is dominated not by the water radiolysis products (mostly radicals) listed above but particles of a different nature, hydroxonium ions H_3O^+, where the term hydroxonium refer to protonated water molecules. This modification of the mechanism of primary radiobiological effects is in good agreement with experimental data. In particular, the extremal dependence of the relative biological efficiency (RBE) of radiations on their ionizing energy losses is accounted for in quantitative terms, as is the increase in the RBE in the relativistic energy range.**

V M Byakov, S V Stepanov Russian Federation State Scientific Center 'Alikhanov Institute for Theoretical and Experimental Physics', ul. B. Cheremushkinskaya 25, 119218 Moscow, Russian Federation
Tel. (7-495) 129 97 51
E-mail: vsevolod.byakov@itep.ru, sergey.stepanov@itep.ru

Received 28 April 2005, revised 13 December 2005
Uspekhi Fizicheskikh Nauk **176** (5) 487 – 506 (2006)
Translated by Yu V Morozov; edited by A M Semikhatov

1. Introduction

The present review is designed to discuss how ionizing radiation exerts its biological action (or starts to exert it, to be precise) as it passes through a living system.

The biological effects of ionizing radiation, such as cell death, radiation burns, or lethality in animals, were described very soon after the discoveries by Roentgen (1895) and Becquerel (1896).

Radiation biology came into being as a purely qualitative science, but the quantitative component had emerged before it came to celebrate its 30-year history in 1924. The 'absorbed dose – biological effect' law was formulated to describe the probabilistic character of the action of ionizing radiation on living systems. In a somewhat simplified form, this law is given by the exponential expression (see Fig. 1)

$$\frac{\mathcal{N}}{\mathcal{N}_0} = \exp\left(-\frac{\mathcal{D}}{\mathcal{D}_{37}}\right), \tag{1}$$

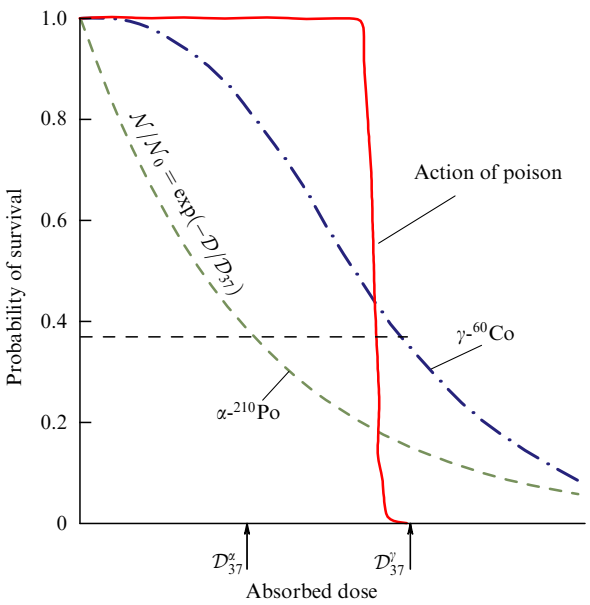

Figure 1. The plot of the survival rate versus the absorbed dose. The exponential dependence of the survival probability (dashed curve) is characteristic of strong ionizing radiations. For weak ionizing radiations (dashed-dotted curve), the dependence deviates from the exponential law. The solid line shows survival after intake of poisons. The absorbed dose of a poison is its mass (the lethal KCN dose is 0.12 g for humans).

where $\mathcal{N}_0$ is the number of animals, bacteria, and other biological phenomena (erythrocytes, enzymes, viruses) prior to irradiation and $\mathcal{N}$ is the number of surviving individuals that absorbed a radiation energy dose $\mathcal{D}$, i.e., the amount of energy per unit body mass. The $\mathcal{N}/\mathcal{N}_0$ ratio is called the 'survival probability.' This word combination should not always be understood in the strict sense. For example, 'survival' in the case of enzyme irradiation simply means the ratio of biological activities before and after the action of ionizing radiation. [1]

The exponential dependence of the survival rate on the absorbed dose is usually apparent in the case of strong ionizing radiations (fast neutrons, α-particles, heavy ions, etc.). These forms of ionizing radiation are characterized by a linear energy transfer (LET) $\gg 1$ eV Å^{-1}, with a change in the dose rate having no effect on the survival rate. The shape of the 'radiation dose – effect' curve is somewhat different from the exponential one in the case of weak ionizing radiations (fast electrons, γ-rays, and X-rays), with LET $\approx (0.02-0.2)$ eV Å^{-1}; it approaches the exponential shape as the dose rate decreases [1].

The dose $\mathcal{D}_{37}$ whose absorption leaves 37% of the affected animals or humans alive within the next 30 and 45 days, respectively, is referred to as the *mean lethal* dose [2, 3]. For the majority of animals irradiated by γ-rays or fast electrons, the mean lethal dose does not exceed 10 Gy ($= 10^4$ erg g^{-1} $= 6.2 \times 10^{16}$ eV g^{-1} $= 2.4 \times 10^{-3}$ cal g^{-1}). Such a dose of ionizing radiation entering an organism causes the ionization of a single molecule per ten million. But it suffices to kill the organism. The thermal equivalent of the lethal dose is insignificant, 0.002 °C; therefore, many authors of radiobiological works regard death under the effect of ionizing radiation as enigmatic [2, 3]. Interestingly, the number of cyanide ions in the human body following intake of a lethal dose of potassium cyanide (0.12 g) is comparable with the ionization rate produced by a lethal dose of ionizing radiation. [2]

The lethal dose of radiations other than γ-rays and fast electrons may be significantly (sometimes, by an order of magnitude) smaller than that. In other words, one dose of strong ionizing radiation produces a much more serious biological effect. The notions of biological efficiency (BE^i) and relative biological efficiency (RBE^i) have been introduced to enable the comparison of the effects of different forms of ionizing radiation (i). The biological efficiency is defined as the inverse of the lethal dose: BE$^i \propto 1/\mathcal{D}_{37}^i$. The relative biological efficiency is the ratio of BE^i to the BE of standard radiation (i.e., γ-radiation of ^{60}Co):

$$\mathrm{RBE}^i = \frac{\mathcal{D}_{37}^{\gamma}}{\mathcal{D}_{37}^i} \,. \tag{2}$$

Figure 2 shows relative biological efficiencies of various types of ionizing radiation acting on different organs and organisms. The RBE values are represented as a function of the LET of ionizing particles or ionizing power of radiations, $-\mathrm{d}E/\mathrm{d}x$. It can be seen that the relation between RBE and LET is not simple and has an extreme character. At LET ≈ 10 eV Å^{-1} (corresponding to α-particles with the energy ≈ 10 MeV), RBE has maximum values that are sometimes one order of magnitude higher than the γ-radiation of ^{60}Co.

2. The development of modern notions concerning mechanisms of radiobiological action

In the 1940s, radiation biology found itself closely associated with another outcome of Becquerel's and Roentgen's discoveries — radiation chemistry, specifically with the part of it dealing with the radiolysis of water, i.e., water decomposition under the action of ionizing radiation. At that time, it was believed that the radiobiological action starts from the initiation of radiochemical processes in the cellular water of living organisms. This hypothesis looked logical from the physical standpoint. Indeed, ionizing radiation penetrating living tissue, where water content amounts to 70% or more, must first of all interact with their aqueous component. [3] Ionization appears to play a key role in this process, giving rise to ion – electron pairs undergoing rapid transformation into longer-lived products (mostly radicals, i.e., molecules having unpaired electrons and therefore highly active chemically) [6, 7]:

$$\mathrm{H_2O} \rightsquigarrow \mathrm{H_2O^{+\cdot}} + \mathrm{e^-} \,.$$

[1] The 'radiation dose – effect' curve is quite different from similar curves describing the effects of various chemical agents, e.g., poisons (see Fig. 1). There is a threshold dose of a poisonous substance below which it exhibits no visible effect. Lethality increases jump-like as soon as the concentration of the poison even slightly exceeds the threshold dose. In contrast, the radiation effect grows slowly as the absorbed dose increases and reflects the response of the living organism to the small variation in dosage.

[2] One-time systemic irradiation by γ-rays or fast electrons at a dose above 1 Gy causes acute radiation sickness. The lethal dose that leads to the death of 50% of higher organisms within one month after the action of radiation varies from 2.5 to 4 Gy [3].

[3] Water makes up 70% of human body weight, with 49% localized inside cells, 17% in extracellular fluids, and 4% in blood plasma. Blood is 92% water and 8% dissolved substances (colloids, ions, complexes). It contains 100 – 200 water molecules per molecule (ion) of dissolved substance [5].

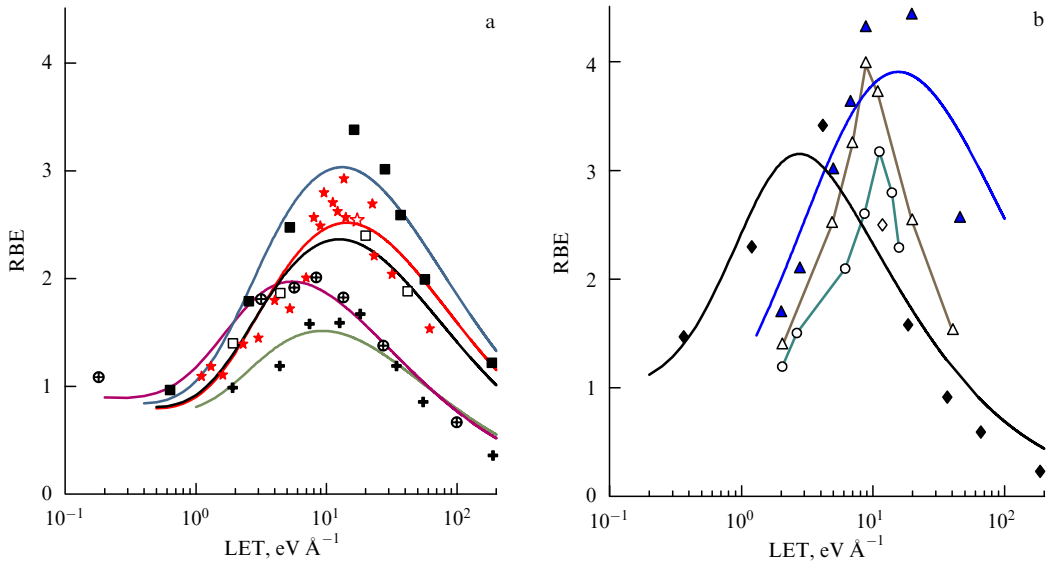

Figure 2. Relative biological efficiency (RBE) as a function of the linear energy transfer (LET) in different organs and organisms affected by ionizing radiation [4]: ■ — human T-1 cell (3.4), ★ — human T-1 cell (3.7), □ — HeLa (3.2), ⊕ — human T-1 cell (1.3), + — CH2B$_2$ (2.4), ▲ — Chinese hamster V-79 (3.9), ◆ — human lymphocytes (0.4), △ — human fetal lung, ○ — CFU-S in vivo. RBE reaches a maximum at LET ≈ 10 eV Å^{-1}. Smooth curves are constructed from Eqn (38). Values of the parameter $\mathcal{L}$ (in eV Å^{-1}) entering (38) are given in parentheses.

An ionized water molecule loses the electron that binds the proton and the oxygen atom. The molecule with the broken bond is no longer able to keep the proton, which becomes embedded in a negatively charged cloud of the intact electron pair in the nearest water molecule. This very rapid process leading to the protonation of the neutral molecule and the formation of a hydroxonium ion and an OH radical is called the *ion–molecular reaction*. The reaction lasts less than 10^{-12} s from the moment of ionization:[4]

$$H_2O^{+\cdot} + H_2O \rightarrow OH^{\cdot} + H_3O^{+}\,. \tag{3}$$

The formation of H_3O^+ ions during water radiolysis was demonstrated by Kabakchi, Kudryashov, and Bugaenko [8], who irradiated aerated weakly alkaline solutions of pH-indicators by short pulses of electrons accelerated to several MeV.[5] They found that an electron pulse generated an acidic form of the indicator that testified to the formation of hydroxonium ions.

Thermalization of a hot electron knocked out as a result of ionization takes approximately as much time as the ion–molecular reaction (< 1 ps). The water molecule exhibits negative affinity to electrons. This means that a traveling electron finds a nanocavity containing a properly oriented water molecule and stays in it, becoming a hydrated electron (e^-_{aq}):

$$e^- + (H_2O)_n \rightarrow e^-_{aq}\,.$$

The hydrated electron is able to absorb a photon with the energy about 2 eV, whereupon it moves to an excited state. This allows detecting such an electron from the characteristic optical absorption spectrum. The important role of the hydrated electron has been demonstrated (since its discovery by E Hart and J Boag in 1962) in many chemical and biological conversions [6, 9].

It is impossible to definitively predict the fate of electrons released into the intracellular medium under the action of ionizing radiation. In all probability, solvated electrons occur in cytoplasm, but their formation in the nucleus is less likely because of the high concentration and reactivity of nucleic acids and proteins with respect to solvated electrons [9].

In aerated water, e^-_{aq} gives rise to a superoxide anion (O^-_2) that also performs an important biochemical function:

$$e^-_{aq} + O_2 \rightarrow O^-_2\,, \tag{4}$$

$$O^-_2 + H_3O^+ \rightleftharpoons HO_2 + H_2O\,, \tag{5}$$

$$OH + OH \rightarrow H_2O_2\,. \tag{6}$$

Reactions of these particles with intracellular biological molecules (denoted as R$\mathcal{B}$) produce bioradicals[6] R$\dot{\mathcal{B}}$(−H), i.e., [10]

$$R\mathcal{B} + OH \rightarrow R\dot{\mathcal{B}}(-H) + H_2O\,,$$

$$R\mathcal{B} + HO_2 \rightarrow R\dot{\mathcal{B}}(-H) + H_2O_2\,,$$

$$R\mathcal{B} + H_2O_2 \rightarrow R\dot{\mathcal{B}}(-H) + H_2O + OH\,.$$

Here and hereinafter, the symbol $\mathcal{B}$ denotes any biologically important functional chemical group and $\mathcal{B}$(−H) is the functional group that lost its H atom.

Intracellular water contains high concentrations of biological molecules R$\mathcal{B}$, typically characterized by a lowered ionization potential. Therefore, the reaction of indirect

[4] The ion–molecular reaction proceeds not only in water but also in other media. For example, methanol may contain a protonated molecule of alcohol and a methoxylic radical:

$$(CH_3OH, CH_3OH) \rightsquigarrow (CH_3OH, CH_3OH)^+ + e^-\,,$$

$$(CH_3OH, CH_3OH)^{+\cdot} \rightarrow CH_3OH^+_2 + CH_2OH^{\cdot}\,.$$

[5] An *indicator* is a chemical compound changing color at different pH values.

[6] The radical R$\dot{\mathcal{B}}$(−H) is the residue of an R$\mathcal{B}$ molecule after it has lost an H atom.

ionization of biological molecules (7) competes, in a way, with ion – molecular reaction (3). In the former reaction, an electron is transported from the dissolved compound to the solvent [11, 7]:

$$H_2O^{+\cdot} + R\mathcal{B} \rightarrow H_2O + R\dot{\mathcal{B}}^{+*}. \quad (7)$$

An appreciable difference between the ionization potentials of biological molecules and water accounts for a greater probability of the electron transfer to the cation-radical $H_2O^{+\cdot}$ from deeper orbitals (with energies approximating the water ionization potential) than from the upper orbital of the biomolecule $R\mathcal{B}$. The asterisk in $R\dot{\mathcal{B}}^{+*}$, as usual, denotes the electron-excited state of the ion. An excess excitation energy of $R\dot{\mathcal{B}}^{+*}$ ions being produced allows their fragmentation via the breakage of C – C and C – O bonds. The proof of such processes is paramount for radiation biology, where current concepts of radiation damage and protection mechanisms are still based on the account of the reactions of radical and molecular products of water radiolysis.

The above reactions are only the initial steps in the long sequence of biochemical transformations.

Thus, physical arguments have led to a concept that the radiobiological action is largely an indirect one and that primary radiobiological effects are most frequently produced by the radical products of the radiolysis of water, first and foremost, by OH and O_2^- radicals, hydrated electrons (e^-_{aq}), and hydrogen peroxide molecules (H_2O_2).

The importance of this concept, known as *the indirect radiobiological action theory*, is difficult to exaggerate. In 1924, it brought Walter Dale to the discovery of two tremendously significant phenomena. One was the possibility of chemically protecting an organism from ionizing radiation by administering certain substances that were thought at that time to scavenge radicals. The other was the amplification effect, that is, enhanced sensitivity to ionizing radiation following the administration of radiosensibilizing chemical compounds. This theory has become an integral element of modern views on the primary radiobiological action [2, 12, 3]. [7]

But it became clear in the course of time that some important questions are difficult to answer in the framework of these views.

• Why does the protective action of radioprotectors manifest itself at concentrations that are obviously too small to enable these agents to effectively scavenge radicals?

• Why does RBE first grow with increasing LET, reach a maximum value at LET ≈ 10 eV Å^{-1}, and drop thereafter (see Fig. 2)?

• Why does RBE increase for ultrarelativistic particles [13]?

• What is the possible cause of the carcinogenic activity of ionizing radiations?

• Why are chemical transformations so small that they are difficult to detect in nonbiological systems after the absorption of a radiation dose lethal to humans (~ 5 Gy) (see [6, p. 240])?

This situation stimulated the search for other factors that might be helpful in explaining the observed peculiarities of the radiobiological action.

It appears that the direct radiobiological action theory fails to adequately account for the above and some other facts because it places too much emphasis on the role of radicals while disregarding the ability of radiolytic products of a different nature to produce biological effects.

In what follows, we present an attempt to modify current notions by demonstrating that the main role in the primary radiobiological action is played by particles other than radicals, that is, by hydroxonium ions (H_3O^+) or, roughly speaking, by protonated water molecules. Unlike radicals, these ions contain only paired electrons. [8]

It is well known that biological structures and processes are highly susceptible to variations in the concentration of hydroxonium ions in liquid water [14]. Effects exerted by these ions are highly important. They include, among others:

• the breakage of hydrogen bonds, the disintegration of the ordered supramolecular structure of biological molecules and their resulting denaturation, that is, the transformation into disordered coils without a definite spatial pattern, accompanied by the loss of biological activity [14, 15]; [9]

• the neutralization of the electric charges of biocolloid anions and stimulation of their coagulation (under physiological conditions, biocolloids exist in a dissociated state, i.e., as anions [16]);

• the suppression of enzyme action;

• acid catalysis (which is so common in organic reactions that it cannot be disregarded in a discussion of the structure and reactivity of biological molecules).

The possible role of hydroxonium ions in radiobiological effects was conjectured by the famous James Frank half a century ago [10]. True, his ideas were rather vague, which may explain why they passed unnoticed. Indeed, virtually all published monographs and textbooks concerning the primary radiobiological action avoid discussing the role of hydroxonium ions, which is not even mentioned among the biologically significant products of water radiolysis (see, e.g., [2, 3, 12]). References [17, 18, 7] appear to have been the first publications dealing with this subject. They were followed in later years by many journal papers and conference reports [19 – 22]. A somewhat different aspect of the influence of acidity on biological processes was discussed in the works of Eidus [23] and Sukhorukov (see [24] and the references therein).

[7] A competing alternative theory assigns a major role to the direct interaction of ionizing radiations with biological molecules (see Ref. [3]). This is the so-called direct action model. It is not considered in this review confined to the merits and demerits of the indirect radiobiological action theory and arguments that can probably contribute to its improvement. We believe that the concept of indirect radiation action lays the foundation for the correct understanding of the mechanism of primary radiobiological action.

[8] We recall that hydroxonium ions emerge as a result of a process stably maintained in liquid water, i.e., spontaneous decomposition of water molecules with the mean lifetime of several hours: $(H_2O, H_2O) \rightleftharpoons H_3O^+ + OH^-$.

[9] Denaturation occurs as a very rapid process starting at a certain acid level in an electroneutral solution. A large number of hydrogen bonds need to be broken in order for a protein chain or its large fragments to acquire the freedom necessary for local motions (rotation, bends, or rolling into coils). It is impossible to liberate one link without affecting others. A given link with broken H-bonds remains motionless if the bonds in the adjacent links remain sufficiently strong. Hydrogen bonds are broken and restored reversibly in pure water and in solutions of low-molecular compounds. Therefore, the above effect cannot be detected in such media. But the breakdown of many neighboring hydrogen bonds in protein or nucleic acid molecules may result in the complete disintegration of their initial structure.

3. Primary radiobiological processes in the eye lens

A variety of primary radiobiological processes in different organs of even one organism dictates the necessity to discuss them via the example of a model organ having a virtually uniform structure in which these processes may be supposed to proceed in the simplest form. The lens of the eye appears to be most suitable for the purpose. Ionizing radiation is known to cause opacity of the lens or radiation cataracts [25, 26, 13].

The primary radiobiological effects in the eye lens are usually attributed to the disintegration of sulfhydryl groups in proteins, most of all by the action of the products of water radiolysis such as radicals OH, $O_2^{-\cdot}$ (HO_2) and hydrogen peroxide H_2O_2 [25]:

$$R-SH + OH \rightarrow RS^{\cdot} + H_2O\,, \tag{8}$$

$$R-SH + HO_2 \rightarrow RS^{\cdot} + H_2O_2\,, \tag{9}$$

$$R-SH + H_2O_2 \rightarrow RS^{\cdot} + H_2O + OH\,. \tag{10}$$

But this setting seems to suggest that the cataractogenic activity of strong ionizing radiations should be lower than that of γ-rays and X-rays. Indeed, the yield of disintegrated SH-groups should be proportional to G_{tot} (i.e., the total yield of OH, $O_2^{-\cdot}$, H-radicals, and H_2O_2):

$$G_{tot} = G_{OH} + G_{O_2^-} + G_H + 2G_{H_2O_2} \tag{11}$$

[here, $G_{O_2^-} = G_{e_{aq}^-}$ because of (4)].

The yield of the radical products involved in reaction (11) markedly decreases as LET increases from 0.01 to 10 eV Å^{-1}, while $G_{H_2O_2}$ grows but insignificantly (Fig. 3). As a result, the total yield of G_{tot} decreases substantially. Therefore, the cataractogenic effect of strong ionizing radiations must be smaller than that of γ-rays and X-rays. However, the real picture is quite the opposite, and experimental observations demonstrate an increase in the biological efficiency with growing LET (Fig. 4).

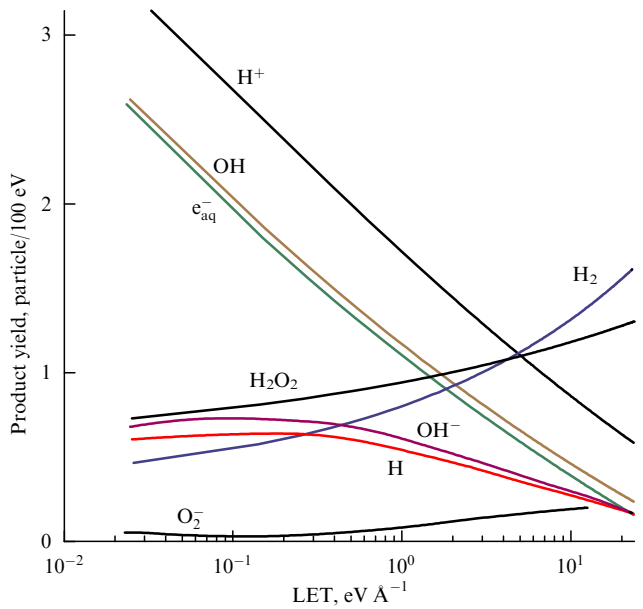

Figure 3. The LET dependence of the yield of various water radiolysis products [27].

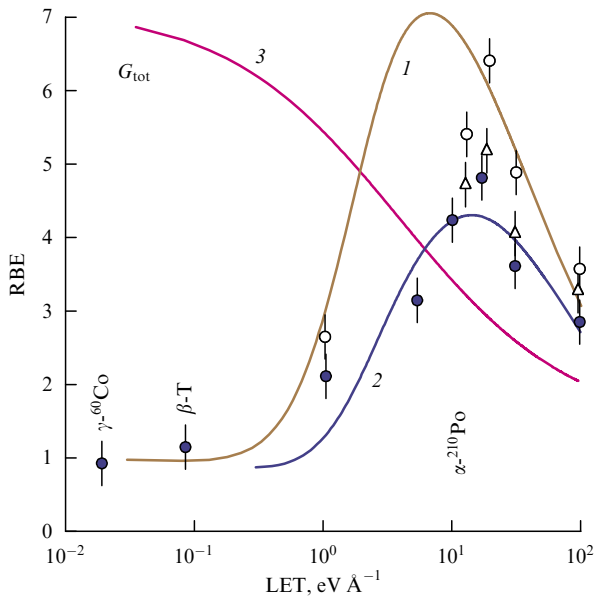

Figure 4. Plots of RBE versus LET at the absorbed doses that differentially damage chromosomes in murine corneal epithelial cells [20% — ○ (1.7), 50% — △, and 63% — ● (3.6)] [26]. Curves *1* and *2* show LET dependences of RBE estimated from Eqn (38) for different severities of chromosomal damage (20% and 63%). Curve *3* is constructed based on Eqn (11) with the data in Fig. 3 taken into account. The values of the parameter $\mathcal{L}$ (in eV Å^{-1}) in Eqn (38) are given in parentheses.

What is the reason then to put forward the hypothesis of enhanced acidity along the tracks of ionizing particles as the main cause of radiation cataracts?

The ophthalmological literature [28] contains numerous facts suggesting that the opacity of the lens and cornea is frequently associated with an increase in the level of hydrogen ions, that is, with local or systemic acidosis. Acidosis is known to develop in a variety of inflammatory eye diseases, local and systemic infections or intoxication, severe diabetes mellitus, and other pathological conditions.

The hypothesis of intratrack enhancement of acidity [18–21] as a cause of radiation cataract [18-21] is first and foremost underlain by the results of an experimental study carried out by Uzbekov [16] at the Ryazanskii Medical Institute.

It is known that the optical media of the eye differ from other tissues and organs of a living organism in that they are characterized by high pH values (7.6–8.0) [28][10]. Their inherent transparency appears to be maintained by enhanced alkalinity. Uzbekov demonstrated that an artificial increase in the hydrogen ion concentration up to $\sim 10^{-5}$ M (pH 5) in the transparent eye tissues of dogs and rabbits (cornea, lens, and vitreous body) *in vitro*[11] and *in vivo* led to their opacity. The author attributed this transformation [16] to the coagulation of proteins and polysaccharides (the principle biological molecules of optical media) and the resulting formation of mucoproteid, a rather stable opaque substance.

Figure 5 illustrates the threshold nature of opacity that develops when the H_3O^+ level exceeds 10^{-5}–10^{-4} M.

[10] pH is a measure of acidity in diluted aqueous and other solutions; the pH value is defined as the negative decimal logarithm of the hydroxonium ion concentration in mol l^{-1} (M).

[11] *in vitro* — 'in glass', in a test tube.

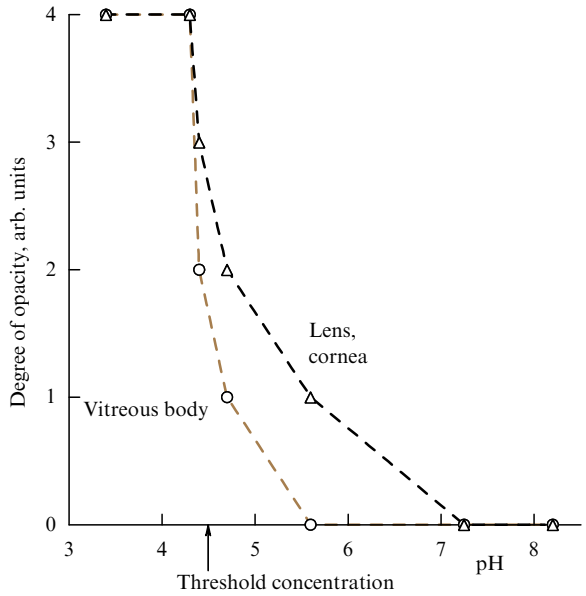

Figure 5. pH dependence of the opacity degree of transparent eye tissues in experiments on artificial enhancement of the hydroxonium ion concentration in the cornea, lens, and vitreous body of dogs and rabbits *in vitro* and *in vivo* [16]. Normal pH $\approx 7.8-8.0$. The opacity has a threshold nature and develops when the H_3O^+ level exceeds $\sim 10^{-5}$ M.

The results of Uzbekov's experiments suggest that intratrack acidity may be a cause of radiation cataracts, but, clearly, if the concentration of hydroxonium ions along the tracks of ionizing particles increase above a certain threshold level [17, 18, 7].

4. Intratrack concentrations of hydroxonium ions

The rapid recombination of charges hampers evaluation of intratrack concentrations of hydroxonium ions in liquid water. It is feasible, however, in vitreous methanol frozen at a low temperature. In this medium, the oxymethyl radicals CH_2OH are practically motionless at the 'nitrogen' temperature (77 K). Because one and the same reaction produces both oxymethyl radicals and oxonium ions $CH_2OH_2^+$ (see footnote 4), the 'immobility' of the former may be used to determine the initial ion concentration by the EPR method. Figure 6 presents the results by Raitsimring, Tsvetkov, and Moralev obtained at the Institute of Chemical Kinetics and Combustion, Novosibirsk, in experiments on local concentrations of oxymethyl radicals in methanol treated with various types of ionizing radiation [29].

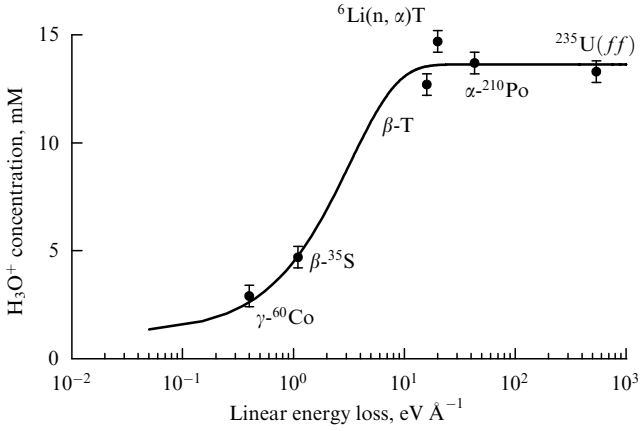

Figure 6. Initial concentration of $CH_3OH_2^+$ ions in the tracks of different ionizing particles in vitreous methanol frozen at 77 K [29].

Before considering the results of the measurements, it seems appropriate to recall the structural features of the track of a fast charged particle [30]. As the particle passes through water, it loses part of its energy in rare head-on collisions. The energy of δ-electrons knocked out in such collisions amounts to hundreds of eV and more. The tracks of these electrons make 'branches' along the trajectory of the primary particle (Fig. 7). The other part of the kinetic energy is lost in numerous sliding collisions. An electron knocked out in a sliding collision usually gives rise to several or dozens of ion – electron pairs inside a spherical nanovolume. In the radiochemical literature, these regions of high ionization density

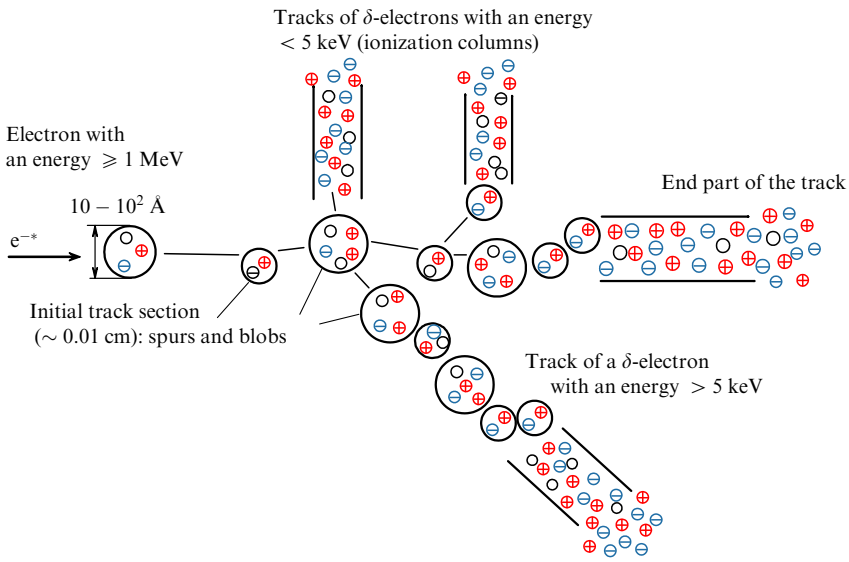

Figure 7. Schematic representation of the track of an ionizing particle in water prior to chemical conversions of primary radiolysis products: H_2O^+, e^-, H_2O^* (a femtosecond time interval counted from the track formation); ○ — H_2O^*; ⊕ — H_2O^+; ⊖ — e^-.

are referred to as *spurs* and *blobs*, depending on their size [31, 6, 7]. While the velocity of a primary particle is sufficiently high ($\sim 10^9$ cm s^{-1}), the average distance between the primary ionization acts is much larger than the spur size; therefore, the spurs are located far apart. In track regions where the velocity of an ionizing particle is comparable to that of atomic electrons, the spurs overlap one another and form cylindrical ionization columns. The relation between the number of ions arising in single spurs and cylindrical columns depends on the particle ionizing power. For example, in the case of fast electrons with the energy ~ 1 MeV, up to 90% of the ions are produced in widely separated spurs and blobs; an opposite picture is observed in the case of α-particles [31].

We now turn to the results of measurements reported by the Novosibirsk group. Identification of the methoxyl radical concentration with that of oxonium ions in Fig. 6 leads to the conclusion that the latter are present in the spurs at about 10^{-3} M; their concentration in the ionization columns of α-particles and fission products increases to 10^{-2} M.

Comparison of these values with the lens opacity threshold established by Uzbekov, $c_{\rm th}(H_3O^+) \sim 10^{-5}$ M, shows that the 'initial' local concentrations of H_3O^+ ions in tracks of charged particles are much higher than the threshold level above which transparent eye tissues become opaque. Therefore, it may be assumed that radiolytic H_3O^+ ions are actually able to cause denaturation and coagulation of biological molecules during irradiation. These processes must occur in all track regions where the ion level exceeds the opacity threshold [17, 18, 7, 20, 22].

5. Formalization of the hypothesis

To make the hypothesis of biological significance of intratrack acidity more specific, we once again turn to the track structure of an ionizing particle (see Fig. 7). The track consists of ion–electron clusters, one part of which (spurs and blobs) have a spheroidal shape and the other (columns) a cylindrical shape. We consider the spatial–temporal evolution of one such cluster, either a spur, a blob, or a cylindrical column. After a time of ~ 1 ps, the cluster comprises three types of radiolytic products: hydrated electrons, OH-radicals, and hydroxonium ions.

Given local electroneutrality in the clusters (which is very likely to occur as far as blobs and columns are concerned [32]), the spatial distributions of e^-_{aq}, H_3O^+, and OH radicals [the latter having a common origin in reaction (3)] must be very similar. Therefore, they can be described in terms of concentration alone:

$$c(\mathbf{r}, t) = c_{H_3O^+} = c_{e^-_{aq}} = c_{OH}\,.$$

It is traditionally assumed [33, 7] that at the initial moment, the concentration has a Gaussian form for both a spherical cluster (spur, blob) of radius a comprising $N^0_{\rm sph}$ particles of all sorts and a cylindrical column of radius b and length L containing $N^0_{\rm cyl}$ OH-radicals and an equal number of ion–electron pairs:

$$c_{\rm sph}(\mathbf{r}, t=0) = c^0_{\rm sph} \exp\left(-\frac{r^2}{a^2}\right), \quad c^0_{\rm sph} = \frac{N^0_{\rm sph}}{(\pi a^2)^{3/2}}\,, \tag{12}$$

$$c_{\rm cyl}(\rho, t=0) = c^0_{\rm cyl} \exp\left(-\frac{\rho^2}{b^2}\right), \quad c^0_{\rm cyl} = \frac{N^0_{\rm cyl}}{\pi b^2 L}, \quad \mathbf{r} = (\rho, z)\,. \tag{13}$$

Being mobile, the particles diffuse from the cluster and react with one another: [12]

$$H_3O^+ + OH^- \to H_2O\,, \tag{14}$$

$$H_3O^+ + e^-_{aq} \to H\,, \tag{15}$$

$$e^-_{aq} + OH \to OH^-\,. \tag{16}$$

The concentration $c(\mathbf{r}, t)$ satisfies the equation

$$\frac{\partial c}{\partial t} = D\Delta c - kc^2 \tag{17}$$

describing diffusion and recombination processes. Here, D is the ambipolar diffusion coefficient ($D \approx D_{H_3O^+} \approx 10^{-4}$ cm^2 s^{-1}). [13] For simplicity, a single constant k is used to characterize the rate of recombination reactions (14)–(16).

In what follows, we need solutions of Eqn (17) for three-dimensional and two-dimensional diffusion. Unfortunately, this equation is nonlinear and allows no analytic solution.

The main simplification usually made to search for an approximate solution in the case of three-dimensional diffusion (spurs, blobs) [33] consists of the assumption that the initial spherically symmetric Gaussian form (12) of the spatial ion distribution persists at all t. This approximation is referred to as the *prescribed diffusion method*. Its application leads to the following expressions for the concentration $c_{\rm sph}(\mathbf{r}, t)$ and the number $N_{\rm sph}(t)$ of H_3O^+ ions in a spur and a blob [7, 18]:

$$c_{\rm sph}(\mathbf{r}, t) = \frac{N_{\rm sph}(t) \exp\left[-r^2/(a^2+4Dt)\right]}{\pi(a^2+4Dt)^{3/2}}\,, \tag{18}$$

where

$$N_{\rm sph}(t) = \frac{N^0_{\rm sph}}{1+\varkappa-\varkappa/\sqrt{1+4Dt/a^2}}\,, \qquad \varkappa = \sqrt{\frac{2}{\pi}}\,\frac{kN^0_{\rm sph}}{8\pi Da}\,. \tag{19}$$

The quantity

$$\frac{N_{\rm sph}(t\to\infty)}{N^0_{\rm sph}} \equiv \frac{N^\infty_{\rm sph}}{N^0_{\rm sph}} = \frac{1}{1+\varkappa} \tag{20}$$

is the fraction of ions that escaped recombination. It differs from zero at any finite value of $\varkappa$. It follows from (19) that the majority of the recombination acts occur at the early stages of diffusion. When the spur linear size increases by a factor of 10, recombination is practically completed. [14]

[12] Reactions (4) and (5), which are also inherent in the aerated intracellular medium, last $> 10^{-7}$ s and therefore play no part in intratrack processes.

[13] We note that the ambipolar diffusion coefficient equals the doubled diffusion coefficient of the least mobile ions [32]. In the present case, such ions are represented by hydrated electrons and hydroxyl ions with similar diffusion coefficients ($D_{OH^-} \approx D_{e^-_{aq}}$) that are half the diffusion coefficient of hydroxonium ions.

[14] For a cylindrical cluster ($\sqrt{4Dt} \ll L$), the prescribed diffusion method gives the following expression for the number $N_{\rm cyl}(t)$ of ions preserved with time t [34]:

$$N_{\rm cyl}(t) = N^0_{\rm cyl}\left[1+\frac{kN^0_{\rm cyl}}{8\pi DL}\ln\left(1+\frac{4Dt}{b^2}\right)\right]^{-1}.$$

This expression is not satisfactory because it always gives $N_{\rm cyl}(t) \to 0$ as $t \to \infty$, inrespective of how small the coefficient $kN^0_{\rm cyl}/(8\pi DL)$ is.

We believe that a better approach to the case of a cylindrical track ($\sqrt{4Dt} \ll L$) has been proposed in Ref. [35], where it is postulated that the concentration of ions is given by the expression

$$c_{\rm cyl}(\rho, t) = \frac{N^0_{\rm cyl}}{\pi(4Dt + b^2)L} \exp\left(-\frac{\rho^2}{4Dt + b^2}\right) \times \left[1 + kt\,\frac{N^0_{\rm cyl}}{\pi(4Dt + b^2)L} \exp\left(-\frac{\rho^2}{4Dt + b^2}\right)\right]^{-1}. \quad (21)$$

This expression is actually an interpolation of two exact solutions of Eqn (17), one at $k = 0$ and the other at $D = 0$ [36]. Integrating Eqn (21) over the volume yields the expression for the number of ions that escaped recombination by time t:

$$N_{\rm cyl}(t) = \frac{\pi(4Dt + b^2)L}{kt} \ln\left[1 + \frac{kN^0_{\rm cyl}t}{\pi(4Dt + b^2)L}\right]. \quad (22)$$

An important feature of Eqn (22) is that the fraction of unrecombined H^+ ions remains, generally speaking, finite as $t \to \infty$:

$$N_{\rm cyl}(t \to \infty) \equiv N^\infty_{\rm cyl} = \frac{4\pi DL}{k} \ln\left(1 + \frac{N^0_{\rm cyl}k}{4\pi DL}\right) = N^0_{\rm cyl}\,\frac{\ln\left[1 + N^0_{\rm cyl}k/(4\pi DL)\right]}{N^0_{\rm cyl}k/(4\pi DL)}. \quad (23)$$

Moreover, the absolute number of particles that escaped recombination grows logarithmically with an increase in the linear loss of energy by a primary particle ($N^0_{\rm cyl}/L \propto$ LET). Formula (23) fairly well describes LET dependences of the yields of water radiolysis products ($e^-_{\rm aq}$, OH).

It follows from (21) that the ion concentration in a cylindrical ionization column can be approximated, at large times [$t \geqslant b^2/(4Dt)$], by the Gaussian function

$$c_{\rm cyl}(\rho, t) \approx N^\infty_{\rm cyl}\,\frac{\exp\left[-\rho^2/(4Dt + b^2)\right]}{\pi(4Dt + b^2)L}. \quad (24)$$

The meaning of this result is straightforward. Recombination of H_3O^+ ions with electrons and OH^- ions mostly proceeds at small times [$t \leqslant b^2/(4Dt)$] as long as the concentration of the particles is low. At larger times, the probability of encounter decreases rapidly ($\propto c^2$), and a further decrease in the concentration of H_3O^+ ions is largely due to their diffusion. The value of the normalization constant is chosen such that integrating (24) over volume gives the correct number of ions that escaped recombination in the track, that is, the number defined by expression (23). In what follows, the behavior of the H_3O^+ concentration at sufficiently large times may be of interest; therefore, the simplified expressions for $c_{\rm sph}(\mathbf{r}, t)$ and $c_{\rm cyl}(\rho, t)$ are used below instead of (18) and (21):

$$c_{\rm sph}(\mathbf{r}, t) \approx N^\infty_{\rm sph}\,\frac{\exp\left[-r^2/(4Dt + a^2)\right]}{\pi(4Dt + a^2)^{3/2}},$$

$$c_{\rm cyl}(\rho, t) \approx N^\infty_{\rm cyl}\,\frac{\exp\left[-\rho^2/(4Dt + b^2)\right]}{\pi(4Dt + b^2)L}.$$

We must now find the volumes $V^{\rm sph}_{\rm th}(t)$ and $V^{\rm cyl}_{\rm th}(t)$ of the clusters in which the concentration $c(\mathbf{r}, t)$ of H_3O^+ ions exceeds the given value of $c_{\rm th}$ (Uzbekov's opacity threshold for the eye lens); in such clusters, biological transformations (denaturation, coagulation, etc.) must occur. Setting $c_{\rm sph}(\mathbf{r}, t) = c_{\rm cyl}(\rho, t) = c_{\rm th}$ in Eqns (18) and (24) and expressing r^2 and ρ^2 from them as

$$r^2 = (4Dt + a^2)\,\ln\frac{N^\infty_{\rm sph}}{\left[\pi(4Dt + a^2)\right]^{3/2}c_{\rm th}}, \qquad \rho^2 = (4Dt + b^2)\,\ln\frac{N^\infty_{\rm cyl}}{\pi(4Dt + b^2)Lc_{\rm th}}, \quad (25)$$

we obtain the respective volumes $V^{\rm th}_{\rm sph}$ and $V^{\rm th}_{\rm cyl}$ of the spherical and cylindrical ion clusters with an over-threshold concentration of H_3O^+ ions:

$$V^{\rm th}_{\rm sph}(\theta) = V^0_{\rm sph}\left[(1 + \theta)\,\ln\frac{c^\infty_{\rm sph}}{c_{\rm th}(1 + \theta)^{3/2}}\right]^{3/2}, \quad (26)$$

$$V^0_{\rm sph} = \frac{4\pi a^3}{3}, \qquad c^\infty_{\rm sph} \equiv \frac{N^\infty_{\rm sph}}{\pi^{3/2}a^3}, \qquad \theta = \frac{4Dt}{a^2},$$

$$V^{\rm th}_{\rm cyl}(\Theta) = V^0_{\rm cyl}(1 + \Theta)\,\ln\frac{c^\infty_{\rm cyl}}{c_{\rm th}(1 + \Theta)}, \quad (27)$$

$$V^0_{\rm cyl} = \pi b^2 L, \qquad c^\infty_{\rm cyl} \equiv \frac{N^\infty_{\rm cyl}}{V^0_{\rm cyl}}, \qquad \Theta = \frac{4Dt}{b^2}.$$

Here, θ and Θ are dimensionless characteristic times of track expansion; $c^\infty_{\rm sph}$ and $c^\infty_{\rm cyl}$ are the 'initial' concentrations of H_3O^+ ions in the cylindrical and spherical clusters.

In the course of time, the volumes $V^{\rm th}_{\rm sph}(\theta)$ and $V^{\rm th}_{\rm cyl}(\Theta)$ first expand to reach a maximum and thereafter shrink to a point. This occurs when

$$\theta_{\max} = \left(\frac{c^\infty_{\rm sph}}{c_{\rm th}}\right)^{2/3} - 1, \qquad \Theta_{\max} = \frac{c^\infty_{\rm cyl}}{c_{\rm th}} - 1, \quad (28)$$

respectively.

The temporal evolution pattern of the volume $V^{\rm th}_{\rm cyl}(\Theta)$ is shown in Fig. 8 for different threshold concentrations $c_{\rm th}$ of H_3O^+ ions. During the lifetime of this volume (hundreds of nanoseconds[15]), hydroxonium ions exert their damaging action. Evidently, the denaturation rate (the number of biomolecules undergoing denaturation per unit time) proportional to the reaction volume $V^{\rm th}_{\rm cyl}(\Theta)$ first increases, reaches a maximum, and then vanishes as the over-threshold volume disappears. The resulting biological effect (in the present case, the number of denaturated molecules) for a cylindrical cluster must be proportional to the integral

$$\Omega^{\rm th}_{\rm cyl} = \frac{b^2}{4D}\int_0^{\Theta_{\max}} V^{\rm th}_{\rm cyl}(\Theta)\,{\rm d}\Theta, \quad (29)$$

and for a spherical cluster, to the integral

$$\Omega^{\rm th}_{\rm sph} = \frac{a^2}{4D}\int_0^{\theta_{\max}} V^{\rm th}_{\rm sph}(\theta)\,{\rm d}\theta. \quad (30)$$

In the framework of the above approximations, calculation of these 4-volumes encounters no difficulty:

$$\Omega^{\rm th}_{\rm cyl} = \Omega^0_{\rm cyl}\int_0^{\Theta_{\max}} (1 + \Theta)\,\ln\frac{c^\infty_{\rm cyl}}{c_{\rm th}(1 + \Theta)}\,{\rm d}\Theta = \frac{\Omega^0_{\rm cyl}(\sigma^2_{\rm cyl} - 2\ln\sigma_{\rm cyl} - 1)}{4},$$

[15] According to Figs 4 and 6, $c_{\rm th} \approx 3 \times 10^{-5}$ M and $c_{\rm cyl} \approx 10^{-2}$ M. Setting $D \approx 10^{-4}$ cm^2 s^{-1} and $b \approx 30$ Å gives $t_{\max} \approx 10^{-7}$ s.

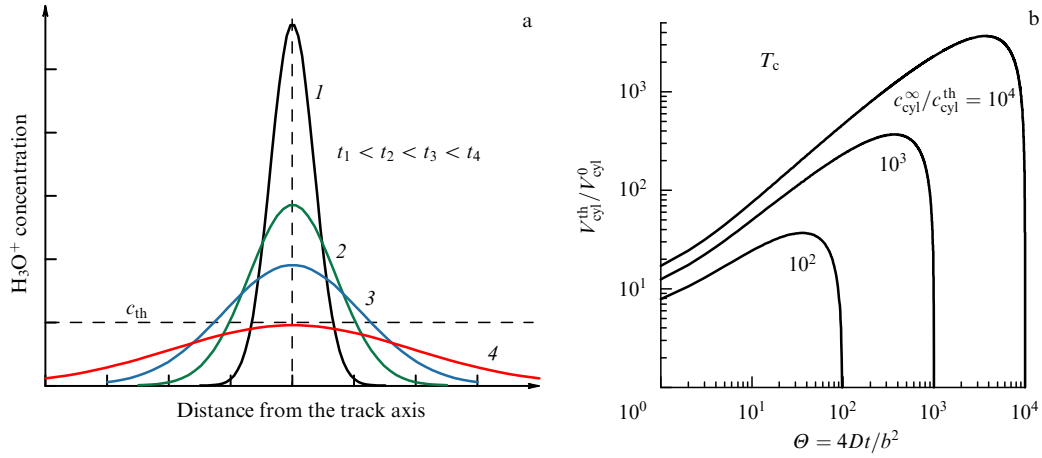

Figure 8. (a) Intracellular spatial – temporal distribution of hydroxonium ions [18, 7]; (b) time-related evolution of the normalized over-threshold volumes V^{th}_{cyl}/V^0_{cyl} in (27) corresponding to different values of the ratio $c^{\infty}_{cyl}/c^{th}_{cyl}$ (10^2, 10^3, and 10^4); at $\Theta = 0$, $V^{th}_{cyl}/V^0_{cyl} = \ln(c^{\infty}_{cyl}/c_{th})$.

where

$$\Omega^0_{cyl} = V^0_{cyl}\,\frac{b^2}{4D} = \pi b^2 L\,\frac{b^2}{4D}\,, \qquad \sigma_{cyl} = \frac{c^{\infty}_{cyl}}{c_{th}}\,.$$

Bearing in mind that $\sigma_{cyl} \gg 1$, we can keep only the first term in the expression for Ω^{th}_{cyl}:

$$\Omega^{th}_{cyl} \approx \frac{\Omega^0_{cyl}\sigma^2_{cyl}}{4} = \frac{\Omega^0_{cyl}}{4c^2_{th}}\left(\frac{N^{\infty}_{cyl}}{\pi b^2 L}\right)^2 = \frac{N^0_{cyl}}{4kc^2_{th}}\,\frac{\ln^2(1+z)}{z}\,, \qquad (31)$$

where

$$z = \frac{kN^0_{cyl}}{4\pi DL} = \frac{\mathrm{LET}}{\mathcal{L}}\,, \qquad \frac{1}{\mathcal{L}} = \frac{k}{4\pi DW}\,. \qquad (32)$$

Here, $N^0_{cyl}W/L = \mathrm{LET}$ and W is the ionization work, i.e., the average energy consumed to produce an ion – electron pair. Various types of ionizing particles do not seem to differ in terms of W values [37].

Similarly, for the 4-volume of a spherical spur (blob),

$$\begin{aligned}\Omega^{th}_{sph} &= \Omega^0_{sph}\int_0^{\theta_{max}}\left[(1+\theta)\,\ln\frac{c^{\infty}_{sph}}{c_{th}(1+\theta)^{3/2}}\right]^{3/2}\mathrm{d}\theta \\ &= \frac{2\Omega^0_{sph}}{3}\,\sigma^{5/3}_{sph}\int_0^{\ln\sigma_{sph}} x^{3/2}\exp\left(-\frac{5x}{3}\right)\mathrm{d}x \\ &\approx \frac{2\Omega^0_{sph}}{5}\,\sigma^{5/3}_{sph}\left[\frac{3^{5/2}\sqrt{\pi}}{4\cdot 5^{3/2}} - \frac{\ln^{3/2}\sigma_{sph}}{\sigma^{5/3}_{sph}}\right], \qquad \ln\sigma_{sph} \gg 1\,,\end{aligned} \qquad (33)$$

where

$$\Omega^0_{sph} = \frac{4\pi a^3}{3}\,\frac{a^2}{4D}\,, \qquad \sigma_{sph} = \frac{c^{\infty}_{sph}}{c_{th}}\,.$$

Considering only the first term in the expansion of Eqn (33) in large σ_{sph} and taking expressions (26) into account gives

$$\begin{aligned}\Omega^{th}_{sph} &\approx \frac{\sqrt{\pi}}{2}\left(\frac{3}{5}\right)^{5/2}\Omega^0_{sph}\left(\frac{c^{\infty}_{sph}}{c_{th}}\right)^{5/3} \approx \\ &\approx \frac{1}{c^2_{th}}\,\frac{N^0_{sph}}{4k}\,\frac{\varkappa}{(1+\varkappa)^2}\left(\frac{c_{th}}{c^{\infty}_{sph}}\right)^{1/3}.\end{aligned} \qquad (34)$$

We now turn to one of the 'primary' charged particles of type i that bombard a living organism and that initially had a kinetic energy E. It may be a fast electron, accelerated ion, α-particle, etc. Let f^i_{cyl} be the part of its energy spent to produce cylindrical ionization columns at the end of the primary particle track and the tracks of δ-electrons; the remaining part $(1 - f^i_{cyl})$ is spent to form spheroidal spurs and blobs along the entire track length, including the tracks of δ-electrons created by the particle. The total 4-volume corresponding to the ith particle is the sum of two terms:

$$\Omega^{th}_i = v^i_{sph}\Omega^{th}_{sph} + v^i_{cyl}\Omega^{th}_{cyl} = \frac{E(1-f^i_{cyl})}{WN^0_{sph}}\,\Omega^{th}_{sph} + \frac{Ef^i_{cyl}}{WN^0_{cyl}}\,\Omega^{th}_{cyl}\,. \qquad (35)$$

The first one, $(v^i_{sph}\Omega^{th}_{sph})$, is the total four-dimensional volume of all spherically symmetric ion clusters (spurs and blobs) numbering $v^i_{sph} = E(1-f^i_{cyl})/(WN^0_{sph})$ that are produced by the primary particle and δ-electrons; the other $(v^i_{cyl}\Omega^{th}_{cyl})$ is the total volume of all cylindrical ionization columns whose total number is $v^i_{cyl} = Ef^i_{cyl}/(WN^0_{cyl})$.

6. 'Absorbed dose – biological effect' relation

The knowledge of the space – time volume Ω^{th}_i permits deducing, in the framework of the above notions, the relation between the absorbed radiation dose and its primary biological effect that agrees, in terms of shape, with the basic 'survival – absorbed dose' law (1) of radiation biology [18, 7]. For this, the fraction φ_i of the irradiated volume V in which the concentration of H_3O^+ ions is above the threshold value c_{th} must be determined:

$$\varphi_i(c_{th}) = \frac{m\Omega^{th}_i}{Vt} = \frac{\mathcal{D}\Omega^{th}_i\delta}{Et}\,, \qquad \mathcal{D} = \frac{mE}{V\delta}\,.$$

Here, $t \gg t_{max}$ is the irradiation time, δ is the mean irradiation density, and $\mathcal{D}$ is the dose absorbed as a result of the formation of m tracks of ionizing particles with the initial energy E (in the case of irradiation by γ-rays or fast neutrons, E is the average energy of primary Compton electrons and recoil nuclei, respectively).

In compliance with the results of Uzbekov's experiments, $\varphi_i(c_{th})$ is taken as a measure of the biological efficiency of the

ith-type ionizing radiation [18, 7]:

$$\mathrm{BE}^i \propto \varphi_i\,.$$

If τ is the characteristic denaturation time of a biological molecule localized in the high-acidity region, the probability of denaturation of any biomolecule in a volume V for time $\mathrm{d}t$ is $\varphi_i(c_{\mathrm{th}})\,\mathrm{d}t/\tau$. Then, a change in the number $\mathcal{N}$ of intact biomolecules is [16]

$$\mathcal{N} = \mathcal{N}_0 \exp\left(-\frac{\varphi_i t}{\tau}\right) = \mathcal{N}_0 \exp\left(-\frac{\mathcal{D}}{\mathfrak{D}_{37}^i}\right),$$

$$\mathfrak{D}_{37}^i = \frac{E\tau}{\Omega_i^{\mathrm{th}}\delta} = W\tau\left(\frac{1-f_{\mathrm{cyl}}^i}{N_{\mathrm{sph}}^0}\,\Omega_{\mathrm{sph}}^{\mathrm{th}} + \frac{f_{\mathrm{cyl}}^i}{N_{\mathrm{cyl}}^0}\,\Omega_{\mathrm{cyl}}^{\mathrm{th}}\right)^{-1}, \qquad (36)$$

where $\mathfrak{D}_{37}$ is the mean 'lethal' dose written with Eqn (35) taken into account. Although the form of Eqn (36) coincides with Eqn (1) describing the exponential 'absorbed dose – biological effect' law, the two equations are not identical. Equation (36) characterizes the action of radiation absorbed by a living system before it responds to the impact. In contrast, Eqn (1) and the values of the lethal dose $\mathcal{D}_{37}^i$ experimentally found using it long after the irradiation characterize the combined effect of ionizing radiation and the response of the organism.

7. Quantitative LET dependence of RBE. Comparison with experiment

Evidently, the comparison of the above quantitative relations with experimental data is subject to some reservation because the theory [Eqns (36) and (37)] refers to the initial phase of the radiobiological process, whereas the resultant biological injury is due as well to events at its subsequent stages.

The problem of correct comparison with experiment pertains to any mechanism of primary biological action, not only the one discussed in this review. As far as one can judge, this problem has not received a fully satisfactory solution. What can be regarded as a specific measure of primary action? There is no general answer to this question. A finite action is a simpler issue. Its measure is a fraction of dead organisms, cells, inactivated enzymes, etc. But what are the effects to be recorded at an intermediate stage, e.g., 10^{-7} s after the onset of irradiation (see footnote 14)?

The present-day situation in radiation biology is reminiscent of that in radiation chemistry in the 1960s, before the advent of pulse radiolysis systems with a picosecond time resolution. At that period, the sole possibility of judging about primary processes was to compare corollaries from one theoretical model or another as regards the yield of final radiolysis products (H_2, H_2O_2, O_2) in pure water and in the presence of chemically active admixtures. The advent of pulse radiolysis enabled researchers to follow the temporal evolution of intermediate radiolytic products.

[16] We note that τ can hardly be identified with the disintegration time of the initial protein chain structure, which may be much longer because of high macroviscosity of the intracellular medium. It is more appropriate to associate τ with the time interval during which the induced process of hydrogen bond breakdown (characterized by considerably lower viscosity) becomes irreversible.

As follows from the derivation of Eqn (36), it defines a fraction of biological injuries (e.g., denaturated molecules) caused by primary radiobiological effects rather than the relative number of organisms dying, e.g., 30 or 45 days after the irradiation.

In comparing expression (36) with the experimentally found relation (1) describing the dependence of survival on the absorbed dose, we suggest, following Eidus (see Ref. [23]), a direct correlation between the number of primary lesions and delayed recorded effects. Evidently, consideration of 'final' radiobiological effects as a criterion for the validity of theoretical models of the *primary* radiobiological action is open to criticism. However, there is no real choice today.

In what follows, we show that such a relation actually takes place in very many cases (see Figs 2, 4, 10; increased RBE for ultrarelativistic particles). This experimental fact appears to indicate that local falls in pH regarded here as a main primary process predetermine, in a way, the final effect of ionizing radiation.

We consider two fast charged particles, a Compton electron produced by a γ-quantum emitted from the radioactive nucleus of ^{60}Co and a certain i-particle (an accelerated ion) having the same energy but different mass and electric charge. Both particles give rise to an equal number of ion – electron pairs within their tracks (because the mean energy of ionization W appears to be similar for different types of ionizing particles); however, these pairs show different spatial distribution patterns. Ions in the track of a fast Compton electron are concentrated in spheroidal spurs and blobs. In the track of the ith particle with a higher LET, many ions, if not most of them, are localized in cylindrical columns.

The expressions for lethal doses $\mathfrak{D}_{37}^{\gamma}$ and $\mathfrak{D}_{37}^{i}$ corresponding to these forms of radiation are given by Eqn (36). By combining their ratio with formulas (31) and (34), we obtain the expression

$$\mathrm{RBE}^i \equiv \frac{\mathfrak{D}_{37}^{\gamma}}{\mathfrak{D}_{37}^{i}} = \frac{(1-f_{\mathrm{cyl}}^i) + f_{\mathrm{cyl}}^i\left(\dfrac{\Omega_{\mathrm{cyl}}^{\mathrm{th}}/N_{\mathrm{cyl}}^0}{\Omega_{\mathrm{sph}}^{\mathrm{th}}/N_{\mathrm{sph}}^0}\right)_i}{(1-f_{\mathrm{cyl}}^{\gamma}) + f_{\mathrm{cyl}}^{\gamma}\left(\dfrac{\Omega_{\mathrm{cyl}}^{\mathrm{th}}/N_{\mathrm{cyl}}^0}{\Omega_{\mathrm{sph}}^{\mathrm{th}}/N_{\mathrm{sph}}^0}\right)_{\gamma}}$$

$$= \frac{(1-f_{\mathrm{cyl}}^i) + f_{\mathrm{cyl}}^i\,\dfrac{(1+\varkappa)^2}{\varkappa}\left(\dfrac{c_{\mathrm{sph}}^{\infty\gamma}}{c_{\mathrm{th}}}\right)^{1/3}\dfrac{\ln^2(1+z)}{z}}{(1-f_{\mathrm{cyl}}^{\gamma}) + f_{\mathrm{cyl}}^{\gamma}\,\dfrac{(1+\varkappa)^2}{\varkappa}\left(\dfrac{c_{\mathrm{sph}}^{\infty\gamma}}{c_{\mathrm{th}}}\right)^{1/3}\dfrac{\ln^2(1+z_{\gamma})}{z_{\gamma}}}\,, \qquad (37)$$

where the parameter $\varkappa$ [see (19) and (20)] characterizes the fraction of H_3O^+ that escaped recombination in spurs. It may be related to the initial yield of water ionization during γ-radiolysis of aqueous solutions [i.e., the number of ion – electron pairs (≈ 6) arising from the absorption of 100 eV of γ-radiation energy] and to the yield of H_3O^+ ions [≈ 3 ion/(100 eV)] that escaped recombination in spurs [6] measured during γ-radiolysis of aqueous solutions. Substitution of these values in (20) gives $\varkappa \approx 1$. In expression (37), $z = \mathrm{LET}/\mathcal{L}$ and $z_{\gamma} = \mathrm{LET}_{\gamma}/\mathcal{L}$, where LET_{γ}, assumed to equal 0.4 eV Å^{-1}, characterizes deceleration of an electron with an energy below 5 keV, whose track has the form of a continuous ionization column (see Figs 7 and 9).

The coefficient $\mathcal{L}$ introduced in Eqns (32) is composed of D, W, and the effective rate constant k characterizing

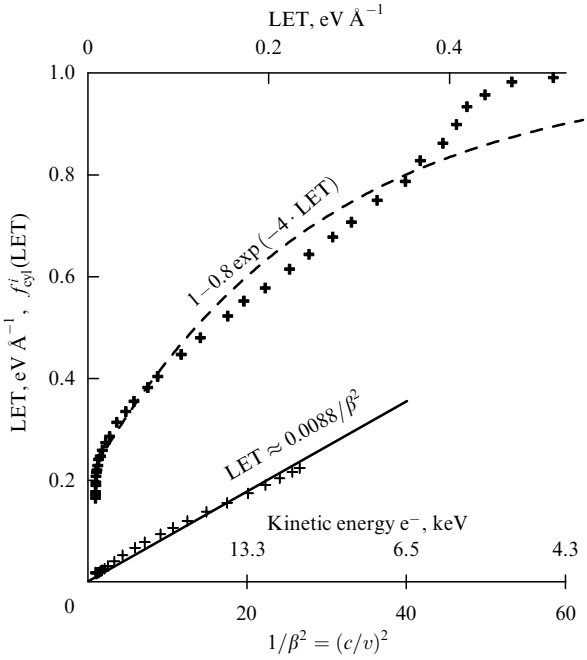

Figure 9. The dependence of the fraction f^i_{cyl}(LET) of the energy of an ionizing particle i consumed to produce cylindrical ionization columns on the initial loss of particle energy; f^i_{cyl}(LET) is derived from the data in Ref. [31], v is the electron velocity, and c is the speed of light.

recombination of hydroxonium ions with OH^- and e^-_{aq}; it gives the following a priori estimate:

$$\mathcal{L} = \frac{4\pi D(\mathrm{cm^2\,s^{-1}})\,W\,(\mathrm{eV})\,N_A}{k\,(\mathrm{litr\ (mol\ s^{-1})})\cdot 10^3}$$

$$\approx \frac{4\pi\cdot 10^{-4}\cdot 17\cdot 6\cdot 10^{23}}{4.3\cdot 10^{10}\cdot 10^3} \approx 3\ \mathrm{eV\ Å^{-1}}$$

(N_A is the Avogadro number). Here, it is assumed that neither the ambipolar ion diffusion coefficient D nor the ionization work W is substantially different from their respective values in ordinary water ($D \approx 10^{-4}$ cm^2 s^{-1}, $W \approx 17$ eV) [7], and the effective rate constant characterizing recombination of hydroxonium ions with OH^-_{aq} and e^-_{aq}, $k \approx 4.3\times 10^{10}$ M^{-1} s^{-1}, is chosen as the geometric mean of the values

$$k(H_3O^+ + e^-_{aq}) \approx 2.4\times 10^{10}\ \mathrm{M^{-1}\,s^{-1}}$$

and

$$k(H_3O^+ + OH^-_{aq}) \approx 8\times 10^{10}\ \mathrm{M^{-1}\,s^{-1}}$$

[38–41]. The resulting value of $\mathcal{L}$ gives

$$z_\gamma = \frac{\mathrm{LET}_\gamma}{\mathcal{L}} \approx 0.13\,.$$

In accordance with the data in Figs 5 and 6, $(c^\infty_{sph}/c_{th})^{1/3} \sim 5$. The values of the coefficients f^γ_{cyl} and f^i_{cyl} are found from Fig. 9 showing the dependence of f^i_{cyl} on LET. It is deduced from the dependence $f^i_{cyl}(K)$ found in Ref. [31] for an ionizing electron ($K = mc^2/(1-v^2/c^2)^{1/2} - mc^2$ is its kinetic energy) and from the data on the stopping power of water [31, 42].

The function f^i_{cyl}(LET) is fairly well approximated by the function $f^i_{cyl} \approx 1 - 0.8\exp\left[-4\,\mathrm{LET\ (eV\,Å^{-1})}\right]$. It follows from Fig. 9 and the results in [42] amending the data in Ref. [31] that $f^\gamma_{cyl} \approx 0.1-0.2$. We finally conclude that the second term in the denominator of (37) may be omitted.

At LET > 0.4 eV Å^{-1}, $f^i_{cyl} \approx 1$. This constraint substantially simplifies Eqn (37):

$$\mathrm{RBE}^i \approx 4\left(\frac{c^\infty_{sph}}{c_{th}}\right)^{1/3} \frac{\ln^2(1+z)}{z}$$

$$= 4\left(\frac{c^\infty_{sph}}{c_{th}}\right)^{1/3} \frac{\ln^2(1+\mathrm{LET}/\mathcal{L})}{\mathrm{LET}/\mathcal{L}}\,. \qquad (38)$$

Evidently, the dependence of RBE on LET is of an extreme character. The condition for the RBE maximum is given by

$$\frac{2z}{1+z} \approx \ln(1+z)\,.$$

The root of this equation (besides the trivial $z = 0$) is $z_{max} \approx 4$. Its substitution in expression (32) gives the position of LET at which RBE has the maximum value: $\mathrm{LET}_{max} \approx 4\mathcal{L} \approx 4\cdot 3 \approx 12$ eV Å^{-1}.

Thus, it may be concluded, on the assumption of the closeness of the parameters D, W, and k for ordinary and intracellular water, that the model under consideration on the whole correctly predicts the value of LET corresponding to the maximum RBE (see Figs 2 and 4). The dispersion of LET_{max} values is naturally attributed, for example, to different diffusion coefficients of hydroxonium ions in different organs and tissues or to the difference in the recombination rate constants k, which are also sensitive to variations in the physico-chemical properties of the medium.

The highest $\mathrm{RBE}^i \approx 10-20$ are obtained in experiments investigating the effects of ionizing radiation on the chromosomal apparatus and gonads [1]. These values fairly well agree with the expression

$$\mathrm{RBE}_{max} \approx 2.6\left(\frac{c^{0\gamma}_{sph}}{c_{th}}\right)^{1/3} \approx 10$$

following from (38) if the threshold and intraspur concentrations of hydroxonium ions are taken to be $c_{th} \approx 10^{-5}$ M and $c^{0\gamma}_{sph} \approx 10^{-3}$ M, as follows from the above experiments [16] and [29].

Smaller values in Figs 2 and 4 are most likely due to the possible reactions between hydroxonium ions and their acceptors. These reactions were disregarded in the derivation of the formulas for the 4-dimensional volumes Ω^{th}_{sph} and Ω^{th}_{cyl}, which resulted in their overestimation. Nevertheless, the application of Eqn (38) to the fitting of the experimental data in Figs 2 and 4 gives evidence that in most cases, it fairly well describes the LET dependence of RBE when LET $\gtrsim 1$ eV Å^{-1}. The numerical values of the parameter $\mathcal{L}$ (see Figs 2 and 4) agree with the above estimate. An equally good result is obtained using data on mutation induction (Fig. 10).

The quantitative explanation of the extreme character of the LET dependence of RBE provides an argument in favor of the hypothesis that the local rise in acidity in tissues and organs under the effect of ionizing radiation is the main factor in the mechanism of primary action of charged particles on living organisms.

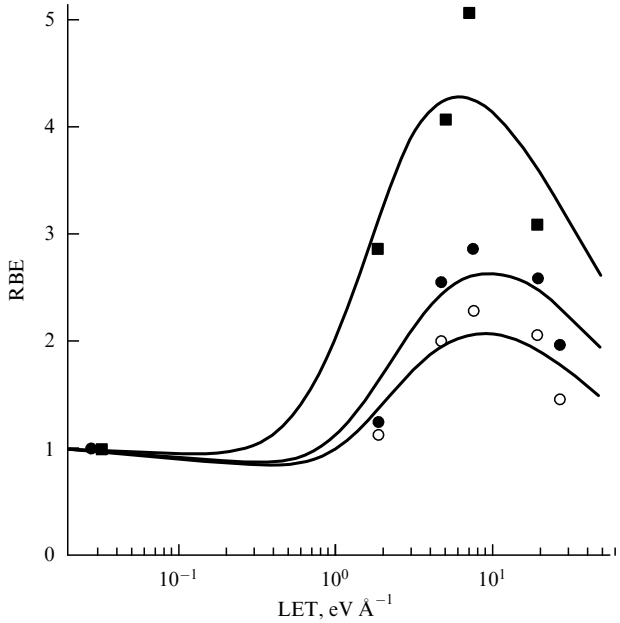

Figure10. LET dependence of RBE of heavy ions estimated from the data on the survival of Chinese hamster cells (○, ●) and induction of mutations (■) [43]. The curves are plotted using Eqn (38). The values of $\mathcal{L}$ (in eV Å^{-1}) are 1.62 (■), 2.56 (●), and 2.34 (○).

8. On the relativistic enhancement of biological efficiency

An important corollary of Eqn (37) concerns the biological efficiency of the emission of ultrarelativistic energies. Frequently cited in the radiochemical literature are the data in [31] on the computed energy distribution between spurs, blobs, and ionization columns that make up the main track of a water-bombarding electron and the tracks of its δ-electrons. These data indicate that an increase in the primary electron energy from 5 keV to 10 MeV is accompanied by an increase in its fraction consumed to form spurs from 60% to 80%, whereas the fraction spent to produce blobs and columns decreases from 40% to 20% [31]. This might suggest a decrease in the biological efficiency with the growth of the primary electron energy. However, such a conclusion would conflict with experimental observations [13]. The cause of the discrepancy lies in the fact that calculations reported in Ref. [31] took only the interactions associated with the ionization and excitation of valence electrons in the medium molecules into account. Although the fraction of such electrons in water and biological molecules is 70 – 80% of the total and they are the least bound ones, the Auger process triggered by the knockout of an electron from the K-shell of a heavy atom (most of all oxygen) makes an appreciable contribution to the biological effect of ionizing radiation [44]. K-ionization of C, N, and O atoms is accompanied by the emission of at least one more electron with a kinetic energy comparable to the energy of the K-level.[17] The knockout of Auger electrons from an oxygen atom leads to the formation of a blob or a short track in its nanovicinity, whose contribution to the biological action [as follows from (37)] is significantly greater than the contribution of spurs with the same total number of ion – electron pairs. This fact distinguishes K-ionizations among others despite their small probability. The Auger effect becomes especially well apparent when the speed of ionizing particles is close to the speed of light. In the ultrarelativistic region, the cross section of the interaction between an ionizing particle and the K-shell of an atom greatly increases [46, 47].[18]

Thus, the cause of the RBE increase with increasing LET is probably the growing overlap between the adjacent spurs and the ensuing increase in the energy spent by ionizing particles to produce continuous ionization columns. The columns are formed by both δ-electrons with energies 500 to 5000 eV [31, 7] and the particle itself when its speed becomes comparable to the speed of such electrons. Despite the seeming absence of an appreciable difference between the number of ion – electron pairs generated by a fast electron and a heavy charged particle per unit energy lost, their 4-volumes are substantially different: $\Omega_{\rm cyl}/\Omega_{\rm sph} \gg 1$. This fact accounts for the different biological effects of these particles. An effect is higher when exerted by heavy particles due, first, to a larger initial concentration of oxonium ions in cylindrical tracks (see Fig. 6) and, second, to a longer time interval during which their over-threshold concentration persists in the cylindrical track [see (28)]. Thus, the most essential biological effects are produced by ionizing collisions in which an energy in the range of 100 to 5000 eV is transferred to the medium electron and which are responsible for the formation of large spurs (blobs) and cylindrical ionization columns (tracks).

However, the role of cylindrical 4-volumes may increase compared with spherical ones not only in the case of radiation with a higher LET due to a decrease in the speed of a fast charged particle down to the Bragg peak. The role of cylindrical 4-volumes also increases as the speed of the particle tends to the speed of light. This situation arises from the markedly increased contribution of K-ionization to the biologically significant energy losses of a relativistic particle.

Indeed, for the above reasons, the radiobiological effect is largely due to collisions associated with the energy transfer in excess of a certain value $Q \geqslant 10^2$ eV, i.e., much higher than the electron bond energy in H atoms and on the L-shells of C, N, and O atoms. These electrons may be regarded as free in collisions of an ionizing particle accompanied by the transfer of an energy higher than Q. The cross section of such collisions (see, e.g., Ref. [49]) is

$$\sigma_{\rm L}(\geqslant Q) = 4\pi\lambda_{\rm e}^2\,\frac{\rm Ry}{Q\beta^2}\,, \tag{39}$$

where $\lambda_{\rm e} = \hbar/(mc) = 3.9\times10^{-11}$ cm is the Compton length of the electron and $\beta = v/c$ is the speed of the bombarding particle in units of the speed of light. As $\beta \to 1$, $\sigma_{\rm L}(\geqslant Q)$ is practically independent of the particle speed.

On the contrary, the cross section of the interaction between an ionizing particle and the K-shell of an atom in the ultrarelativistic region increases substantially [46, 47]:

$$\sigma_{\rm K} = \frac{4\pi\lambda_{\rm e}^2 M_{\rm K}^2}{\beta^2}\left[\ln\frac{2mc^2\beta^2}{1.65\,I_{\rm K}(1-\beta^2)} - \beta^2\right]. \tag{40}$$

[17] The escape probability of an Auger electron upon ionization of an oxygen K-shell is practically unity and that of the emission of an X-ray fluorescence quantum does not exceed tenths of a percent. The spectrum of Auger electrons consists of a few energy lines; the most intense is the line corresponding to the energy 500 eV [45].

[18] Lomanov [48] appears to have been the first to pay attention to the possible role of K-ionization in the relativistic enhancement of RBE (even if from other considerations).

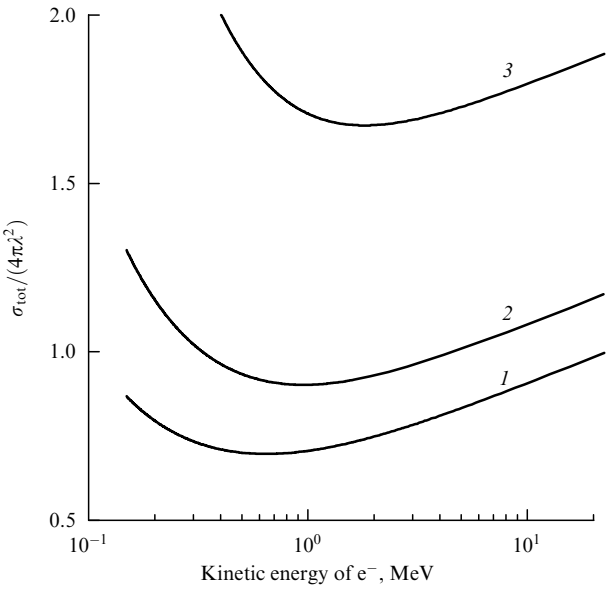

Figure 11. A rise in the percentage of K-ionization with increasing energy of the bombarding electron. Curves *1*, *2*, and *3* correspond to Q values of 540, 290, and 100 eV, respectively [44].

Here, I_K is the K-shell ionization potential,

$$M_K^2 = \int_{I_K}^{\infty} \left(\frac{\mathrm{d}f_K}{\mathrm{d}E}\right) \frac{\mathrm{Ry}}{E}\,\mathrm{d}E\,,$$

and $(\mathrm{d}f_K/\mathrm{d}E)$ is the oscillator differential strength.

Thus, the percentage of K-ionizations increases in the relativistic region. Their relatively small (5–10%) contribution to the absorbed dose allows disregarding interactions with the inner shells of atoms in the computation of energy losses, particle path, etc. But, in conformity with radiobiological effects for which collisions with the energy transfer $\geqslant 10^2$ eV are most essential, ionization of K-shells must be taken into consideration because its contribution is comparable to that of external shells. Indeed, summation of expressions (39) and (40) with weights corresponding to the numbers of electrons on the K and L-shells of H_2O molecules (for oxygen, $I_K = 532$ eV, $M_K = 2.91 \times 10^{-2}$) gives the total cross section σ_{tot} of a collision with an energy transfer in excess of Q:

$$\sigma_{tot} = 8\sigma_L + 2\sigma_K\,. \tag{41}$$

As the energy of the particle increases, σ_{tot} first decreases to a minimum at $\approx 0.5-2$ MeV (the smaller Q is, the higher the energy) and thereafter increases. Figure 11 shows the dependences of σ_{tot} on the electron kinetic energy. It can be seen that K-ionizations may contribute appreciably to the relativistic enhancement of RBE [13]. (Unfortunately, a more detailed discussion of this effect is hampered by the lack of experimental data.)

9. On the mechanism of protective action of radioprotectors

One of the main implications from the conclusion about the dominant radiobiological role of hydroxonium ions is a novel view of the mechanism of protective action of radioprotectors. These agents must more readily react with H_3O^+ ions and their precursors (H_2O^+ cation-radicals) than with radicals.

The aforementioned experiments by Kabakchi, Kudryashov, and Bugaenko [8] on the irradiation of aqueous solutions of pH-indicators were continued at the Institute of Experimental and Theoretical Physics in the 1970s to evaluate the reactive capacity of radioprotectors with respect to hydroxonium ions.[19] The difference from the previous experiments [8] was that a radioprotector (cysteine, cysteamine, or amino-ethylisothiouronium) was added to water, besides a pH indicator. It was expected that the radioprotector would scavenge hydroxonium ions and thus prevent acidification of the pH indicator. The results confirmed the prediction.

The rate constants obtained in these experiments are presented in Fig. 12a. They are one or two orders of magnitude higher than the rate constants characterizing the interaction of radioprotectors with radicals. Moreover, the relations shown in Fig. 12b suggest an inverse correlation between the medically prescribed dosage of a given radioprotector and the rate constant of its reaction with a hydroxonium ion.

Positron spectroscopy appears to be a promising technique for the elucidation of interactions between radioprotectors and cation-radicals [22]. Figure 13 demonstrates experimental results obtained by the Strasbourg positron group [50]. Abbe, Dulpatre, and co-workers used positrons to irradiate amines dissolved in methanol; these compounds are known to show high affinity for protons and to be efficacious acceptors of cation-radicals [51, 52]. At least one of them, aniline, is a radioprotector [53]. Numerous experiments on positron behavior have demonstrated [7] that in many condensed media (including methanol), a positron (e^+) reacts with one of the electrons at the end part of its track, giving rise, with rather high probability, to a positronium atom (Ps):

$$e^+ + e^- \rightarrow \mathrm{Ps}\,.$$

This reaction is frequently suppressed by a competing reaction between track electrons and cation-radicals

$$CH_3OH^+ + e^- \rightarrow CH_3OH^*\,.$$

The addition of aniline into methanol increases the yield of Ps. Aniline transforms cation-radicals into weakly reactive products and thereby undercuts positron competitors for the intratrack electron:

$$CH_3OH^+ + C_6H_5NH_2 \rightarrow CH_3OH + C_6H_5NH_2^+\,.$$

The results of this experiment lay the ground for a discussion of the possibility of interaction of radioprotectors with primary cation-radicals in the living organism.[20]

[19] The experiments were carried out by I G Aksenov, O P Stepanov, F G Nichiporov, V V Chernyshev, E P Kalyazin, and V M Byakov with the ITEP pulse radiolysis unit using a proton beam with the energy around 20 MeV as the source of ionizing radiation. Unfortunately, the results of these experiments have never been published and were only mentioned in Ref. [7].

[20] Cation-radicals $H_2O^{+\cdot}$ may live much longer in the intracellular medium than in ordinary water [22].

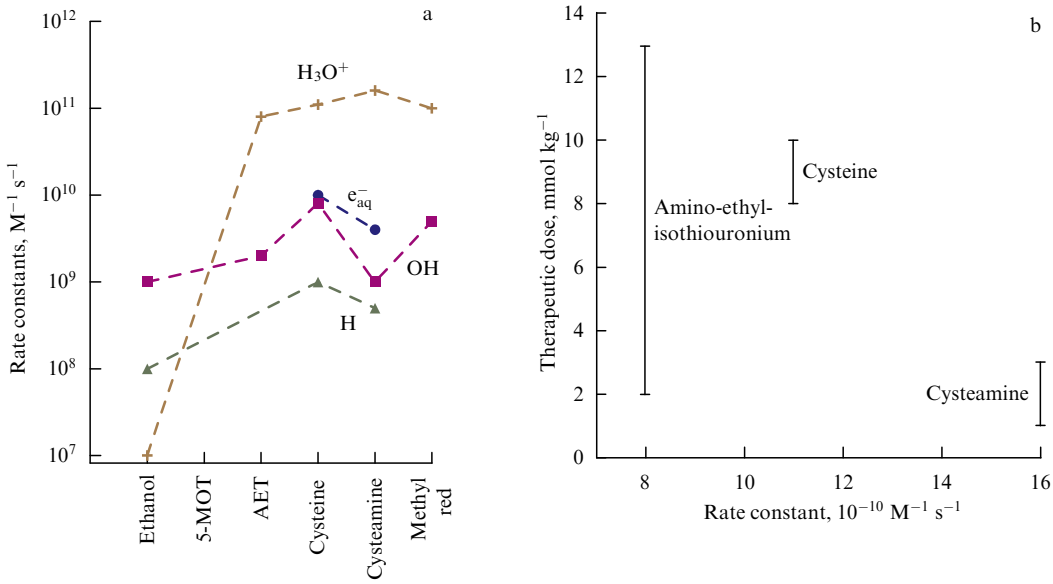

Figure 12. (a) Rate constants of reactions between radioprotectors and intermediate water radiolysis products [7]; (b) correlation between therapeutic doses (mmol kg^{-1}) of radioprotectors recommended by radiobiologists [54] and rate constants of their reactions with H_3O^+ ions.

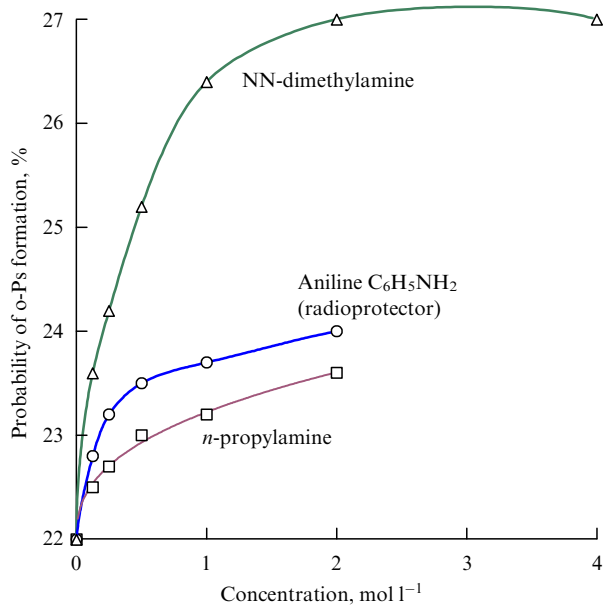

Figure 13. Amplification effect in positronium formation in methanol after the addition of amines [50].

It is well known that molecules of the overwhelming majority of radioprotectors contain amine groups [54]. This notable fact has not thus far attracted much attention.[21] It receives a natural explanation in the framework of the above notions because amines are characterized by very high affinity for protons and at the same time have a low ionization potential compared with water. The enhanced probability of Ps formation in the presence of amines (by virtue of their interaction with cation-radicals) not only confirms the hypothesis ascribing the crucial role to a decrease in pH in the tracks of ionizing particles in the mechanism of their biological action but also provides a guide to searching for their new effective varieties.

[21] Usually, only the presence of the SH group in radioprotector molecules is emphasized.

10. Possible role of H_3O^+ ions in the induction of mutagenic and carcinogenic actions of ionizing radiation

The recognition of the critical contribution of electrophilic hydroxonium ions to primary radiobiological action facilitates the understanding of a most characteristic feature of ionizing radiation, i.e., its ability to produce mutagenic and carcinogenic effects. A starting point for understanding may be the fact that all mutagens and carcinogens, notwithstanding the great variety of them, have one common property: they are strong electrophilic agents, and hence effective acceptors of electron pairs and free electrons [55 – 57]. It is supposed that the primary act of carcinogenesis consists of the interaction between a carcinogen molecule entering the cell nucleus and its DNA. If this is indeed the case, one of the radiolysis products induced by ionizing radiation must be strongly electrophilic. This property is inherent in hydroxonium ions more than in any other water radiolysis product. The recognition of the dominant role of these ions in biological action may be helpful in understanding the mechanisms of mutagenic and carcinogenic effects of ionizing radiation.

It is worth noting in this context that proton pumps functioning on the outer cell membrane and in nuclear and mitochondrial membranes are oriented so as to remove hydroxonium ions from them.

11. Radiobiological paradox

We return to the fundamental problem mentioned in the beginning of this review to which biologists and chemists have not yet received a fully satisfactory solution [3]. That is, why are chemical transformations so small that they are difficult to detect in nonbiological systems after the absorption of a radiation dose lethal to humans ($\sim$ 5 Gy) (see [6, p. 240])?

Although this question appears to interest the authors of almost all books on radiation biology, no one comes to the conclusion that inevitably suggests itself. The fact is ionizing radiation produces much stronger effects in living systems than the traditionally considered chemical reactions involving free radicals.

We consider how the notion of the dominant role of enhanced intratrack acidity helps to resolve this principal radiobiological paradox, that is, the discrepancy between the magnitude of the biological effect and the amount of ionizing radiation energy absorbed by biological tissues.

Up to now, we have disregarded the concrete cell structure when discussing radiochemical reactions in living cells. We simply used a diluted aqueous solution of biological molecules to simulate the intracellular medium. This approach proved useful because it provided a quantitative explanation for the dependence of RBE on LET, the increase in RBE for relativistic particles, and the correlation between the prescribed doses of radioprotectors and their reactive capacity with respect to hydroxonium ions. In a word, it somewhat advanced the understanding of the nature of carcinogenic activity of ionizing radiation.

Now, we have to abandon the idea of cell contents as a homogeneous paste reminiscent of an oil and regard them rather as a juicy fruit jelly larded with small and dense lumps that are frequently very different from the surrounding 'jelly' in terms of structure and composition (Fig. 14).

Cells are extremely diverse in shape, size, and internal structure. At the same time, all of them have a number of common features, such as the presence of a plasma membrane that encloses their contents and a variety of organelles, of which the largest is the globe-shaped nucleus localized in the cell center. Following it in terms of size are mitochondria and lysosomes. These organelles are also enclosed by membranes. The membrane resembles a sandwich in which a lipid portion is placed between two protein layers. Membranes function as if they were pierced with pores through which various substances are transported in either direction.

Lysosomes, discovered by Christian de Duve only in the 1950s, are found in the cells of many (but not all) organs of animals. This discovery provided a happy solution to a puzzle that had long occupied the thoughts of biochemists. Indeed, cell homogenates contain large quantities of enzymes, including some that are able to digest almost all substances that make up the cell structure. It is known that the cell cannot resist the action of any such enzyme in a pure form; hence the puzzle: how do the intact cells avoid the deleterious activity of these enzymes? The fact is they are contained in lysosomes or intracellular particles enclosed by their own outer membrane. The membrane keeps enzymes within the particle and thereby prevents their action on other intracellular components. However, as soon as the cell dies, lysosomal membranes break up and liberate enzymes that rapidly and completely decompose residual cell matter. In other words, lysosome-enclosed enzymes are safe for the intact cell but rapidly destroy diseased and lesioned cells.

It is natural to think that locally enhanced acidity in the tracks of ionizing particles contributes to the destruction of lysosomal membranes. Only a very low energy is needed for the purpose. The effect of a direct membrane injury inflicted by the denaturating action of hydroxonium ions is multiply amplified by the cell's own powerful means of self-destruction in the form of lysosomal enzymes that effectively split vitally important macromolecules, such as proteins, lipids, and nucleic acids. Under normal conditions, this process cannot be realized due to the protective effect of lysosomal membranes that lock hydrolytic enzymes within lysosomes and prevent their interaction with other cell components. When the membranes break up and the enzymes are released inside the cell, they rapidly manifest their deleterious activity and cause damage to the cell within a few minutes after their liberation. Figuratively speaking, hydroxonium ions only open the locks and the released enzymes do the rest.[22]

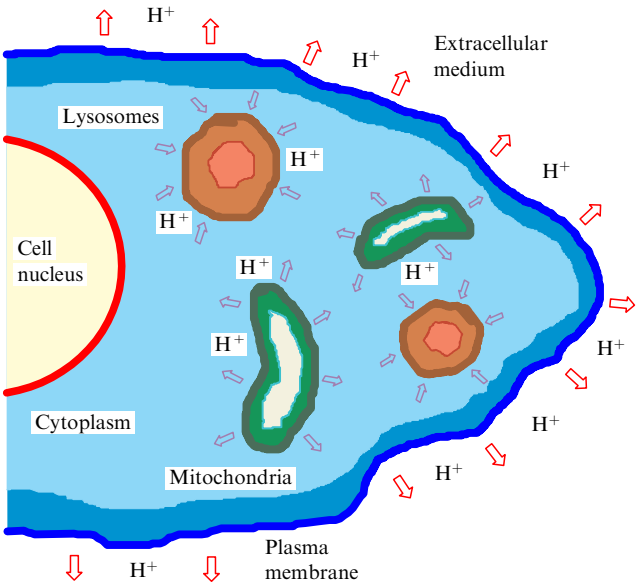

Figure 14. Model of the cell. The nucleus, a storage medium for genetic information, contains proteins, almost all the DNA, some RNA, and enzymes. Mitochondria produce energy and 75% of ATP; they also contain enzymes, substrates for lipid and organic acid oxidation to CO_2, and water. Lysosomes contain enzymes that digest almost all unwanted substances in a diseased or mechanically lesioned cell.

That damage to lysosomal membranes may constitute a trigger mechanism for the cell enzymatic breakdown was first postulated in the monograph by Bacq and Alexander [53], even though the authors did not relate it to the enhancement of intracellular acidity. They regarded injury to the biological membrane as a result of an oxidative chain process with the participation of oxygen.

12. pH, hyperthermia, and 'chocolate' therapy

Almost half a century ago (1963), the well-known German physicist Manfred von Ardenne[23] proposed an original method to manage malignant tumors by heating them to 42 °C while infusing glucose into the systemic circulation [59–62]. Von Ardenne's idea was first met with some scepticism, but in the course of time it raised increasingly greater interest. It turned out that overheating combined with excess glucose is actually fatal for tumor cells. Hydroxonium ions appear to play an important role in this effect.

As shown in experiment, intracellular pH decreases from 7.0 to 6.5 and below as temperature rises to 40–42 °C.

[22] By way of example, inflammatory processes are associated with acidosis and cell lysis whereby lysosomal enzymes break away into the cytoplasm.
[23] In 1945–1955, von Ardenne worked in the USSR; he was awarded a Lenin prize.

Enhanced acidity kills the cell and the released lysosomal enzymes destroy what remains of it.

The majority of malignant cells are more sensitive to high temperature than normal ones because of the intrinsically increased acidity of their internal milieu. Tumors contain cells that undergo a deficit of oxygen because of impaired blood supply, especially if they are localized in the central part of the neoplasm. Such cells generate energy to maintain themselves by glucose cleavage in the process of glycolysis. Lactic acid formed through glycolysis acidifies the intracellular medium. The resulting excess of hydroxonium ions makes the cells thermosensitive.

Interestingly, the cancer cell, unlike the normal one, produces energy through glycolysis even under hypoxic conditions. This ability provides a basis for one more approach to the treatment of malignant tumors known as 'chocolate therapy'. It consists of administering large amounts of glucose into the patient's systemic circulation from which it is actively absorbed by cancer cells. The excess of glucose leads to a decrease in pH; in other words, the cells become increasingly acidified.

Thus, overheating and 'chocolate therapy' cause the self-acidification and death of tumor cells. Some authors tried to combine these modalities with the treatment by ionizing radiation and reported a markedly enhanced therapeutic efficiency of this approach [63, 64].

Here again, pH variations are involved. The cell has specific enzymes to repair radiation damage. Their activity decreases with increasing acidity, which hampers the reparative process. The administration of large amounts of glucose to mice immediately after irradiation, i.e., when it is necessary to suppress reparative enzymes, results in a higher percent of the animals that benefit from the combined therapy compared with those treated by the same doses of ionizing radiation alone.

A series of studies conducted jointly by the Institute of Nuclear Research, Dubna, and the Russian Oncological Research Center, Moscow, [65 – 67] demonstrated the strong lethal action of glucose on tumor cells in hypoxia. Also, a combination of excess glucose and ionizing radiation proved to have additive effect on cancer cells. It was shown that the lethal effect of glucose was due to decreased pH, i.e., self-acidification resulting from intense glycolysis. Neither the method used to diminish pH[24] nor the conditions of oxygenation influenced by themselves the outcome of the treatment. The oxygenation conditions mattered only if the pH was lowered by means of an excessive glucose load. Glycolysis was much more pronounced in hypoxic conditions than under oxygenation.

It is noteworthy that the effects of enhanced acidity in tumor cells, as well as in the eye lens, become apparent only after pH decreases to less than 5.3. This implies a certain threshold value of pH above which 'self-acidification' cannot develop. This explains why excess glucose has practically no effect on properly aerated cells where glycolysis is slowed down and pH decreases only to a value of 5.6, i.e., remains higher than the threshold level [67]. It may be supposed that the threshold nature of induced acidity reported in Ref. [16] has a universal character for various cell types, even though they may differ in sensitivity to pH changes.

[24] A decrease in pH in tumor cells was reached by the administration of buffer solutions, besides glucose.

13. Participation of radiolytic hydroxonium ions in post-track reactions

Previous sections dealt with the effects of hydroxonium ions (denaturation and the like) preconditioned by their initially high intratrack concentrations in excess of a threshold level necessary to maintain the process. Such processes occur in the early (intratrack) phase of irradiation. We once again evaluate the duration of the 'over-threshold' stage and the maximum part (volume) of the organism being irradiated that becomes occupied by H_3O^+ ions at the time of their highest concentration.

The energy absorbed by the organism at a γ-radiation dose of 5 Gy gives rise to $\sim 2 \times 10^{18}$ ion – electron pairs per cubic decimeter. This number decreases by half as a result of intratrack recombination. When the ions are uniformly distributed in a volume they populate (1 dm^3), their concentration is 10^{-6} M, i.e., below the threshold level, $\sim 10^{-5}$ M [16]. This means that the maximum size of the volume that the H_3O^+ ions can occupy without the loss of ability to exert biological action is approximately one tenth of the total volume of a given organism. Assuming that the initial number of ion – electron pairs in a 'typical' spur is 6 and becomes 3 after the intratrack recombination is completed, the volume per spur is 6×10^9 Å^3. The ions remain biologically active while they occupy not more than 1/10 of this volume (6×10^8 Å^3) having the radius $R_{\text{bio}} \approx 500$ Å. Hence, the period during which H_3O^+ ions retain biological activity is $t_{\text{bio}} \approx R_{\text{bio}}^2/D \approx 10^{-7}$ s.

This does not mean, however, that the function of H_3O^+ ions in radiobiological transformations is restricted to intratrack reactions. We try to understand the fate of hydroxonium ions after their local concentration has dropped to below the threshold level. At this moment, it equals $\sim 10^{-5}$ M and is still two orders of magnitude higher than the normal concentration of H_3O^+ ions in most biological tissues.

The intracellular medium of living organisms contains dissolved oxygen formed when a large part of solvated electrons are converted to superoxides, i.e., anion-radicals $O_2^{-\cdot}$. These superoxides most frequently act as mild reducing agents; that is, they release electrons and thus regenerate free oxygen. The presence of hydroxonium ions in a solution results in a change of the chemical form of superoxide anions. $O_2^{-\cdot}$ accepts a proton and turns to radical-acid $HO_2^{\cdot}$. This radical is a true acid because the association of the proton and the superoxide is reversible. Unlike $O_2^{-\cdot}$, its protonated form is an oxidizing, i.e., dehydrating agent. Radical $HO_2^{\cdot}$ is energetically capable of oxidizing any bonds in organic compounds, including those normally resistant in redox reactions [3]. The reaction

$$R\mathcal{B} + HO_2 \rightarrow R\dot{\mathcal{B}}(-H) + H_2O_2$$

is the most common one involving this radical. It results in three bioradicals originating from one $HO_2^{\cdot}$:

$$R\mathcal{B} + H_2O_2 \rightarrow R\dot{\mathcal{B}}(-H) + H_2O + OH\,,$$

$$R\mathcal{B} + OH \rightarrow R\dot{\mathcal{B}}(-H) + H_2O\,.$$

Thus, radiolytic hydroxonium ions multiply increase the number of bioradicals in aerated solutions and impart an oxidative character to the radiobiological process.

14. The role of hydroxonium ions in the development of senile cataracts

In the foregoing, we presented some arguments in favor of the dominant role of intratrack acidity in the radiobiological action, specifically in the development of radiation cataracts. We now turn to the etiology of senile cataracts and clarify whether the affected lens has enhanced acidity and what role it plays in the development of opacity.

The etiology of senile cataracts was addressed in a study conducted by Stroganov of the Gor'kovskii Medical Institute [68 – 70]. This author demonstrated that the development of senile cataracts is associated with a change in the lens elemental composition, most of all with an increase in the Ca, Fe, and Mg content [68] (Fig. 15).

It is worth noting that changes in the elemental composition of the cataractous lens are reminiscent of those in traumatic iridiocyclitis (see Fig. 15) and opposite to age-related changes in healthy eyes [68 – 70]. This fact indicates that senile cataracts are a disease rather than an inevitable consequence of biochemical transformations evolving in the ageing eye.

It is natural to regard the similarity of changes in the lens elemental composition of cataracts and traumatic iridiocyclitis as a manifestation of common biochemical processes in these two pathological conditions. It follows from what is known about the pathogenesis of inflammation that changes in the uveal tract in the case of traumatic iridiocyclitis are underlain by rapidly developing acidosis. The inflamed tissue accumulates acidic metabolites that contribute to lowering pH at the affected site to 4.3 – 3.6 [71, 72]. Then, the decreased pH is the immediate cause of senile lens opacity.

Of primary significance in this context is a 14-fold rise in the Ca content. It is responsible for the impaired permeability of the lens capsule [73] and the resulting decrease in its oxygen supply. As mentioned in a preceding section, a deficit of oxygen in cells promotes the accumulation of partly oxidized metabolic products, including pyruvic and lactic acids that acidify the intracellular medium [15]. There is indeed an age-specific shift of pH to acidic values in the cataractous lens [71]. This implies that senile and radiation cataracts may have a common immediate cause, namely acidosis or an increased concentration of hydrogen ions. In radiation cataracts, this increase takes place in the tracks of ionizing particles and in senile cataracts, most likely in the vicinity of mitochondria where oxidative processes are localized. This line of reasoning helps in understanding the similarity of the element content between the eye tissues affected by cataracts and traumatic iridiocyclitis.

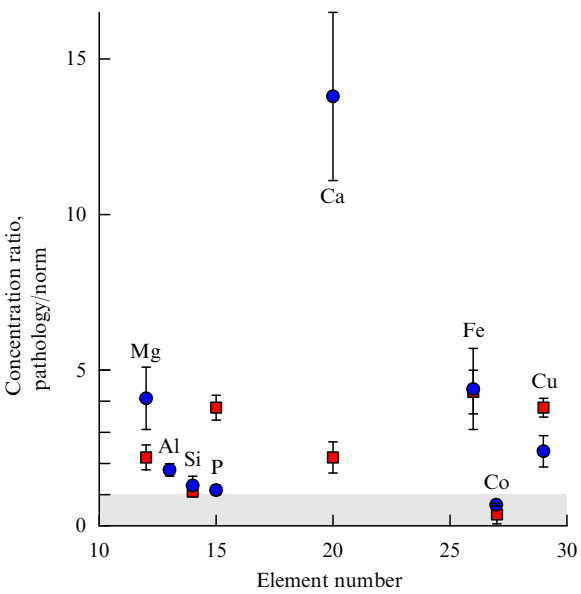

Figure 15. Variation of chemical element contents in the cataractous lens (●) and in the inflamed uveal tract (traumatic iridiocyclitis) (■).

It would appear that a single pharmaceutical product must produce identical effects in either condition. The validity of this supposition was verified by professor Vainshtein of the Gel'mgolts Institute of Eye Diseases, Moscow [74]. This author demonstrated that administration of cysteine (mentioned before as having radioprotective activity and preventing the development of radiation cataracts [75]) into the lens also has a curative effect in senile cataracts. Fairly good results in the treatment of senile cataract were reported by Petrov, an ophthalmologist based in the city of Sochi [76], who administered sodium thiosulfate ($Na_2S_2O_3$) into the lens. According to Ref. [77], $Na_2S_2O_3$ is an acceptor of H_3O^+ ions. Thus, the two examples are in excellent agreement with the idea of the critical role of enhanced acidity in the primary radiobiological action. Moreover, there is reason to believe that thiosulfate possesses radioprotective properties.

15. Conclusion

The primary biological action of ionizing radiation is usually described in terms of chemical reactions involving radical products of intracellular water radiolysis (OH, H, e^-_{aq}, O^-_2, H_2O_2) and bioradicals originating from them or emerging directly. This approach has facilitated the understanding of fundamental phenomena associated with the biological action of ionizing radiations such as protective effects and aggravation of injuries inflicted by chemical additives introduced into the living system. On the other hand, it fails to explain other important facts.

The present review is concerned with one more biological effect of ionizing radiation, i.e., a local increase in acidity along the track of a charged particle in an aqueous solution. The intratrack acidity is several orders of magnitude higher than in ordinary water contained in a living organism. Biological systems are known to be extremely sensitive to variations in acidity. The data presented in this review indicate that the dominant role in the primary biological action of ionizing radiations is played by hydroxonium ions (H_3O^+) or, to put it simply, protonated water molecules, rather than the aforesaid water radiolysis products of a totally different nature (mostly radicals). Hydroxonium ions emerge from the same reactions of water radiolysis that produce OH radicals but, at the same time, they are well-known products of the water molecule decomposition that continuously proceeds in the liquid phase according to reaction

$$(H_2O, H_2O) \rightleftharpoons H_3O^+ + OH^- .$$

The thus modified mechanism of primary radiobiological action

• explains the extreme character of the relation between the LET of ionizing radiations and their relative biological efficiency, correctly predicting the RBE maximum location (≈ 10 eV Å^{-1}) and magnitude (~ 10);

• predicts the RBE increase at relativistic energies of ionizing particles;

• creates a new view of the mechanism of protective action of at least certain radioprotectors (substances exhibiting high reactive capacity with respect to hydroxonium ions or to H_2O^+ cation-radical must have protective properties);

• predicts a correlation between medically prescribed doses of radioprotectors and their reactive capacity with respect to hydroxonium ions;

• offers a natural resolution of the so-called 'radiobiological paradox,' i.e., the manifestation of the biological effect when a very small amount of energy is absorbed by a living organism; and

• provides arguments in favor of acidosis as a common immediate cause of radiation and senile cataracts and traumatic iridiocyclitis.

References

1. Darenskaya N G et al. *Otnositel'naya Biologicheskaya Effektivnost' Izluchenii. Faktor Vremeni Oblucheniya* (Relative Biological Efficiency of Radiations. Radiation Time Factor) (Moscow: Atomizdat, 1968)
2. Dertinger H, Jung H *Molekulare Strahlenbiologie* (Berlin: Springer-Verlag, 1969) [Translated into English: *Molecular Radiation Biology* (Berlin: Springer-Verlag, 1970); translated into Russian (Moscow: Atomizdat, 1973)]
3. Kudryashov Yu B *Radiatsionnaya Biofizika* (*Ioniziruyushchie Izlucheniya*) (Radiation Biophysics (Ionizing Radiation)) (Moscow: Fizmatlit, 2004)
4. Ainsworth E J *Adv. Space Res.* **6** (11) 153 (1986)
5. Williams D R *The Metals of Life: the Solution Chemistry of Metal Ions in Biological Systems* (London: Van Nostrand-Reinhold, 1971) [Translated into Russian (Moscow: Mir, 1975) p. 37]
6. Pikaev A K *Sovremennaya Radiatsionnaya Khimiya. Radioliz Gazov i Zhidkostei* (Modern Radiation Chemistry. Radiolysis of Gases and Liquids) (Moscow: Nauka, 1986)
7. Byakov V M, Nichiporov F G *Vnutritrekovye Khimicheskie Protsessy* (Intratrack Chemical Processes) (Moscow: Energoatomizdat, 1985)
8. Kabakchi S A, Kudryashov L I, Bugaenko L T *Int. J. Radiat. Phys. Chem.* **2** 187 (1970)
9. Hart E J, Anbar M *The Hydrated Electron* (New York: Wiley-Intersci., 1970) [Translated into Russian (Moscow: Atomizdat, 1973)]
10. Nickson J J (Ed.) *Symp. on Radiobiology, 1950. The Basic Aspects of Radiation Effects on Living Systems* (New York: Wiley, 1952)
11. Afanas'ev A M, Kalyazin E P *Kosvennaya Ionizatsiya Veshchestv* (Indirect Ionization of Matter) (Moscow: Znanie , 1989)
12. Amiragova M I et al. *Pervichnye Radiobiologicheskie Protsessy* (Primary Radiobiological Processes) 2nd ed. (Ed. N V Timofeev-Resovskii) (Moscow: Atomizdat, 1973)
13. Fedorenko B S *Fiz. Elem. Chastits At. Yadra* **22** 1199 (1991) [*Sov. J. Part. Nucl.* **22** 586 (1991)]
14. Rose S P R *The Chemistry of Life* (Harmondsworth: Penguin, 1966) [Translated into Russian (Moscow: Mir, 1969)]
15. Pimentel G C, Spratley R D *Chemical Bonding Clarified Through Quantum Mechanics* (San-Francisco: Holden-Day, 1969) [Translated into Russian (Moscow: Mir, 1973)]
16. Uzbekov G A *Voprosy Med. Khim.* **7** 190 (1961)
17. Byakov V M, Kalyazin E P, Afanas'ev A M "Rol' lokal'nykh ponizhenii pH i kosvennoi ionizatsii biomolekul v mekhanizme biologicheskogo deistviya ioniziruyushchikh izluchenii" ("Role of local falls of pH and indirect ionization of biological molecules in the mechanism of biological action of ionizing radiations"), in *IV Mezhd. Biofizicheskii Kongress, 7–14 Avgusta 1972 g. Tezisy Dokladov* (IV Intern. Biophysical Congress, 7–14 August 1972. Abstracts) Vol. 4 (Moscow, 1972) p. 444
18. Byakov V M "Ponizhenie pH v trekakh ioniziruyushchikh chastits i ego vozmozhnaya rol' v pervichnykh radiobiologicheskikh protsessakh" ("Falls in pH in the tracks of ionizing particles and their possible role in primary radiobiological processes"), Preprint ITEP-182 (Moscow: Institute of Theoretical and Experimental Physics of the USSR Acad. of Sci., 1983)
19. Byakov V M et al. *Khim. Vys. Energii* **29** 230 (1995) [High Energy Chem. **29** 211 (1995)]
20. Byakov V M, Stepanov S V *Radiatsionnaya Biologiya. Radioekologiya* **37** 469 (1977)
21. Byakov V M, in *9èmes Journées d'Etudes de Chimie sous Rayonnement* (*JECR-98*), *21–26 juin 1998, Bonascre, France*
22. Byakov V M, Stepanov S V, in *Modern Problems of Nuclear Physics and Physics and Chemistry of Condensed Matter: Proc. of the 7th Intern. Moscow School of Physics, Otradnoe, Moscow Region, Russia, February 16–26, 2004* (Moscow: Academprint, 2004) p. 30
23. Eidus L Kh *Membrannyi Mekhanizm Biologicheskogo Deistviya Malykh Doz. Novyi Vzglyad na Problemu* (Membrane-Based Mechanism of Biological Action of Small Doses. A Novel View of the Problem) (Moscow: Institut Teoreticheskoi i Eksperimental'noi Biofiziki, 2001)
24. Sukhorukov B I, Rybalko L M, Shabarchina L I *Radiobiologiya* **28** (1) 23 (1988)
25. Barron G, in *Symp. on Radiobiology, 1950. The Basic Aspects of Radiation Effects on Living Systems* (Ed. J J Nickson) (New York: Wiley, 1952) p. 249
26. Nevzgodina L V, Grigor'ev Yu G, Marennyi A M *Deistvie Tyazhelykh Ionov na Biologicheskie Ob'ekty* (Action of Heavy Ions on Biological Objects) (Moscow: Energoatomizdat, 1990)
27. Byakov V M, Nichiporov F G *Radioliz Vody v Yadernykh Reaktorakh* (Water Radiolysis in Nuclear Reactors) (Moscow: Energoatomizdat, 1990)
28. Odintsov V P *Kurs Glaznykh Boleznei* (Lectures on Eye Diseases) 5th ed. (Moscow: Medgiz, 1946)
29. Raitsimring A M, Tsvetkov Yu D, Moralev V M *Int. J. Radiat. Chem.* **5** (3) 249 (1973)
30. Miterev A M *Usp. Fiz. Nauk* **172** 1131 (2002) [*Phys. Usp.* **45** 1019 (2002)]
31. Mozumder A, Magee J L *Radiat. Res.* **28** (2) 203 (1966)
32. Stepanov S V, Byakov V M *J. Chem. Phys.* **116** 6178 (2002)
33. Kuppermann A, in *Actions Chimiques et Biologiques des Radiations* Vol. 5 (Ed. M Haïssinsky) (Paris: Masson, 1961) p. 85
34. Jaffe G *Ann. Phys.* (Leipzig) **42** 303 (1913)
35. Wilhelm H E *J. Chem. Phys.* **47** 4356 (1967)
36. Filinovskii V Yu, Chizmadzhev Yu A, in *Trudy I Vsesoyuzn. Soveshchaniya po Radiatsionnoi Khimii* (*25–30 Marta 1957 g.*) (Proc. of the 1st All-Union Conf. on Radiation Chemistry (25–30 March 1957)) (Moscow: Izd. AN SSSR, 1958) p. 19 [Translated into English (New York: Consultants Bureau, 1959)]
37. "Average energy required to produce an ion pair", ICRU Report 31 (Washington, DC: Intern. Commission on Radiation Units and Measurements, 1979)
38. Schmidt K H, Ander S M *J. Phys. Chem.* **73** 2846 (1969)
39. Pikaev A K, Kabakchi S A *Reaktsionnaya Sposobnost' Pervichnykh Produktov Radioliza Vody. Spravochnik* (Reactive Capacity of Primary Water Radiolysis Products) (Moscow: Energoizdat, 1982)
40. Kabakchi S A, Pikaev A K *Dokl. Akad. Nauk SSSR* **275** 106 (1984)
41. Berezhkovskii A M et al. *Dokl. Akad. Nauk SSSR* **307** 625 (1989)
42. Santar I, Bednář J *Int. J. Radiat. Phys. Chem.* **1** (2) 133 (1969)
43. Krasavin E A et al. *Fiz. Elem. Chastits At. Yadra* **35** 1483 (2004) [*Phys. Part. Nucl.* **35** 797 (2004)]
44. Byakov V M, Kalyazin E P *Radiochem. Radioanal. Lett.* **56** (2) 67 (1982)
45. Siegbahn H, Asplund L, Kelfve P *Chem. Phys. Lett.* **35** 330 (1975)
46. Durup J, Platzman R L *Discuss. Faraday Soc.* **31** 156 (1961)
47. Durup J, Platzman R L *Int. J. Radiat. Phys. Chem.* **7** 121 (1975)
48. Lomanov M F, in *Voprosy Mikrodozimetrii. Trudy Pervogo Vsesoyuzn. Soveshchaniya po Mikrodozimetrii* (Problems of Dosimetry. Proc. of the First All-Union Workshop on Microdosimetry) Vol. 1 (Eds V I Ivanov, A N Krongauz) (Moscow: Atomizdat, 1973) p. 107
49. Bete G A, Ashkin Yu, in Experimental Nuclear Physics Vol. 1 (Ed. E Sergè) (New York: Wiley, 1953) [Translated into Russian: "Prokhozhdenie izlucheniya cherez veshchestvo" ("Passage of radiation through matter"), in *Eksperimental'naya Yadernaya Fizika* (Exprimental Nuclear Physics) Vol. 1 (Ed. S Segre) (Moscow: IL, 1955) p. 141]

50. Abbe J Ch et al. *J. Inorg. Nucl. Chem.* **43** 2603 (1981)
51. Warman J M et al. *Chem. Phys. Lett.* **43** 321 (1976)
52. Levay B, Lund S J G, Mogensen O E *Chem. Phys.* **48** 97 (1980)
53. Bacq Z M, Alexander P *Fundamentals of Radiobiology* 2nd ed. (New York: Pergamon Press, 1961) [Translated into Russian (Moscow: IL, 1963)]
54. Kuzin A M *Problemy Radiobiologii* (Problems of Radiation Biology) (Novoe v Zhizni, Nauke, Tekhnike. Ser. Biologiya. Vyp. 1 – 2 (News in Life, Science, Technique. Ser. Biology. Issue 1 – 2)) (Moscow: Znanie, 1970)
55. Miller E C *Cancer Res.* **38** 1479 (1978)
56. Politzer P, Martin F J (Jr) (Eds) *Chemical Carcinogens. Activation Mechanisms, Structural and Electronic Factors, and Reactivity* (Amsterdam: Elsevier, 1988)
57. Bakale G "A Carcinogen-screening test on electrons", in *Linking the Gaseous and Condensed Phases of Matter: the Behavior of Slow Electrons* (NATO ASI Ser., Ser. B, Vol. 326, Eds L G Christophorou, E Illenberger, W F Schmidt) (New York: Plenum Press, 1994)
58. de Duve C *A Guided Tour of the Living Cell* (New York: Scientific American Books, 1984) [Translated into Russian (Moscow: Mir, 1987)]
59. von Ardenne M, Reitnauer P G "Übersauerungs Grenze und pH der Tumorzelle in ihrer Beziehung zur Krebs-Mehrschritt-Therapie" *Acta Biol. Med. Germ.* **25** 483 (1970)
60. *Khim. Zhizn'* (2) (1969)
61. *Khim. Zhizn'* (6) (1970)
62. *Khim. Zhizn'* (10) (1983)
63. Aleksandrov N N et al. *Primenenie Gipertermii i Giperglikemii pri Lechenii Zlokachestvennykh Opukholei* (The Application of Hyperthermia and Hyperglycemia for the Treatment of Malignant Tumours) (Moscow: Meditsina, 1980)
64. Yarmolenko S P *Ukroshchenie Stroptivoi* (The Taming of the Shrew) (Ser. Radiobiologiya — Lyudyam, Vyp. 2) (Moscow: Znanie, 1981)
65. Shmakova N L et al. "Letal'noe deistvie glyukoznoi nagruzki na opukholevye kletki" ("Lethat action of glucose loading on tumor cells"), Preprint P19-85-826 (Dubna: Joint Institute for Nuclear Research, 1985)
66. Shmakova N L et al. "Sovmestnoe vozdeistvie na opukholevye kletki inoniziruyushchikh izluchenii i glyukoznoi nagruzki: sensibilizatsiya, sinergizm i additivnost'" ("Combined effect of ionizing radiations and glucose loading on tumor cells: sensibilization, synergism and additivity"), Preprint P19-85-825 (Dubna: Joint Institute for Nuclear Research, 1985)
67. Shmakova N L et al. "Rol' pH v letal'nom deistvii glyukoznoi nagruzki na opukholevye kletki" ("The role of pH in the lethat action of glucose loading on tumor cells"), Preprint P19-85-827 (Dubna: Joint Institute for Nuclear Research, 1985)
68. Stroganov L M "Soderzhanie khimicheskikh elementov v tkanyakh zdorovykh glaz, ikh dinamika s vozrastom i pri nekotorykh glaznykh zabolevaniyakh" ("Chemical elements contained in healthy eye tissues, their dynamics in ageing and in certain eye diseases"), Author's Abstract of Thesis for Candidate of Medical Sciences (Gor'kii: Medical Institute, 1970)
69. Stroganov L M, in *Primenenie Spektral'nogo Analiza v Biologii i Meditsine* (Application of Specral Analysis in Biology and Medicine) (Gor'kii: Medinstitut, 1970) p. 70
70. Stroganov L M, in *Primenenie Spektral'nogo Analiza v Biologii i Meditsine* (Application of Specral Analysis in Biology and Medicine) (Gor'kii: Medinstitut, 1970) p. 77
71. Shlopak T V *Mikroelementy v Oftal'mologii* (Microelements in Ophthalmology) (Moscow: Meditsina, 1969)
72. Fisher F *Ophthalmologica* **114** 1 (1947)
73. Gifford S R, Lebensohn J E, Puntenny I S *Arch. Ophthalmol.* (Chicago) **8** 414 (1932)
74. Vainshtein E S *Khim. Zhizn'* (11) 76 (1976)
75. Swanson A A, Rose H W, Taube J I *Arch. Ophthalmol.* (Chicago) **59** 465 (1958)
76. Petrov A G "Giposul'fit protiv katarakty" ("Hyposulfite against cataract") *Khim. Zhizn'* (11) 75 (1976)
77. Anan'in A V et al. *Dokl. Akad. Nauk SSSR* **222** 845 (1975)